Donald, Flora; Green, Sarah; Searle, Kate; Cunniffe, Nik J; Purse, Bethan V. 2020. **Small scale variability in soil moisture drives infection of vulnerable juniper populations by invasive forest pathogen.**

The definitive version was published in *Forest Ecology and Management*, 473, 118324. 13, pp. 10.1016/j.foreco.2020.118324

Small scale variability in soil moisture drives infection of vulnerable juniper populations by invasive forest pathogen

Flora Donald[abd], Sarah Green[b], Kate Searle[c], Nik J. Cunniffe[d], Bethan V. Purse[a]

[a]UK Centre for Ecology and Hydrology, Maclean Building, Benson Lane, Crowmarsh Gifford, Wallingford, Oxfordshire, OX10 8BB, UK flodon@ceh.ac.uk beth@ceh.ac.uk

[b]Forest Research, Northern Research Station, Roslin, Midlothian, EH25 9SY, UK sarah.green@forestresearch.gov.uk

[c]UK Centre for Ecology and Hydrology, Bush Estate, Penicuik, Midlothian, EH26 0QB, UK katrle@ceh.ac.uk

[d]Department of Plant Sciences, University of Cambridge, Downing Street, Cambridge, CB2 3EA, UK njc1001@cam.ac.uk

Abstract

The oomycete plant pathogen, *Phytophthora austrocedri*, is an aggressive killer of cypress trees causing severe mortality of Chilean cedar (*Austrocedrus chilensis*) in Argentina since the 1940s and now of common juniper (*Juniperus communis* s.l.) in the UK. Rapid mortality of key UK juniper populations was first observed in the early 2000s. The causal agent of mortality was confirmed as *P. austrocedri* in 2012 and the pathogen has now been widely detected - but is not ubiquitous - in juniper populations across Scotland and England. Although juniper has a broad distribution across the northern hemisphere, the UK incidence of *P. austrocedri* remains the only confirmed infection of juniper populations globally. Juniper is an important species for biodiversity, so it is imperative to understand the abiotic and biotic drivers of emergent *P. austrocedri* infection to inform detection, containment and conservation strategies to manage juniper populations across the full extent of its range.

As management of UK juniper populations is primarily conducted at a local level, we investigated field scale drivers of disease – in three, geographically separate populations with different infection histories. Variation in the proportion of juniper showing symptoms - discoloured or dead foliage – was measured using stratified sampling across along key environmental gradients within each 100-hectare population. Potential predictors of infection included altitude, slope, distance to nearest watercourse, soil moisture (mean percentage volumetric water content), area of red deer browsing damage and area of commonly associated vascular plant species. We assessed support in the data for alternative models explaining the spatial distribution of *P. austrocedri* symptoms using full subset covariate selection and Deviance Information Criteria (DIC). Despite differences in environmental gradients and infection histories between populations, area of juniper symptomatic for *P. austrocedri* increased with waterlogging, increasing with soil moisture in sites where soils had higher peat or clay contents, and decreasing with proximity to watercourses where sites had shallower, sandier soils. Furthermore, we identified common taxa in the associated plant

community that correlated with increased area of symptoms and could be used by land managers as indicators to identify microsites at high risk of infection, enabling site-specific tailoring of disease management strategies. Such strategies could include prioritising detection inspections in microsites with high water tables and high grazing pressure (guided by indicator taxa), limiting soil disturbance in wet microsites and creating sites for natural regeneration in drier microsites, to minimise pathogen spread and maximise the resilience of existing juniper populations.

1.0 Introduction

The frequency of plant pathogen introductions outside their native ranges is increasing as global trade networks expand (Chapman et al., 2017). Successful establishment of pathogens in these new environments is increasingly being facilitated by degradation of the receiving communities through habitat fragmentation, species turnover and land use change (Chapman et al., 2016; Meentemeyer et al., 2011). Economic losses from plant diseases in the natural environment can result directly from drastic reductions in the extent and viability of host species, increased cost of detection and containment measures, or from indirect losses such as destablisiation of ecosystem functioning from loss of biodiversity or negative visual impacts detering tourists, driving down house prices and increasing local crime rates (Boyd et al., 2013; Kovacs et al., 2011; Mills et al., 2011; Troy et al., 2012). While it is appealing to act immediately to try to control disease outbreaks, the effectiveness of these actions improves as more information on the processes governing spread becomes available, often relying on information that does not exist prior to pathogen introduction (Thompson et al., 2018). Understanding the subset of abiotic and biotic conditions in the invaded range under which introduced pathogens are likely to infect susceptible host populations can improve targeting of such interventions and highlight risk factors for outbreaks in uninvaded locations (Cunniffe et al., 2016).

69 The oomycete genus *Phytophthora* contains many pathogenic species that adversely impact
70 plant health, forestry and agriculture, necessitating expensive, long-term, landscape scale
71 management. Between 1970 and 1989, 11 *Phytophthora* species were introduced to China,
72 12 to the UK and 16 to the USA (Barwell et al., in review). In the two decades following, the
73 number of additional species introduced at least doubled in China (20) and the UK (29) and
74 increased five-fold in the USA (54). While not all of these species established, some of them
75 have caused serious tree mortality with dramatic landscape and economic consequences. In
76 Western Australia 282 000 ha of Jarrah (*Eucalyptus marinata*) have been lost to *P. cinnamomi*
77 (Boyd et al., 2013), while trade of Port-Orford cedar (*Chamaecyparis lawsoniana*) in the north-
78 western United States was almost eliminated by *P. lateralis* (Hansen, 2015). Meanwhile,
79 millions of coast live oak (*Quercus agrifolia*) and tanoak (*Notholithocarpus densiflorus*) trees
80 in California and Oregon, and 18 000 ha of Japanese larch (*Larix kaempferi*) in the UK and
81 Ireland have been killed by *P. ramorum* (Meentemeyer et al., 2011; O'Hanlon et al., 2018;
82 Peterson et al., 2014).
83
84 First described in 2007, *Phytophthora austrocedri* has caused widespread mortality of Chilean
85 cedar (*Austrocedrus chilensis*) in Argentina since the 1940s (Greslebin et al., 2007; Greslebin
86 and Hansen, 2010). The pathogen is homothallic and is potentially spread by both asexual,
87 motile zoospores dispersed through any form of moving water, and sexually produced, thick-
88 walled oospores that can remain viable for extended periods of time and be translocated in
89 soil (Green et al., 2015; Henricot et al., 2017). Infection usually starts in the roots before
90 spreading into the cambium and phloem, creating necrotic lesions that can extend to the full
91 width of each layer, starving whole branches, trunks or trees of water and nutrients causing
92 rapid defoliation and mortality (Green et al., 2015).
93
94 Symptoms were first brought to the attention of UK plant pathologists in the mid-2000s, when
95 significant numbers of symptomatic juniper (*Juniperus communis* s. l.) could be observed in
96 two of the larger populations (Glenartney and Haweswater), but *P. austrocedri* was not

97 confirmed as the causal agent of mortality until 2012 following isolation and confirmation of
98 Koch's postulates (Green et al., 2012). In the UK the pathogen is present as a single genetic
99 lineage exhibiting no diversity in nucleic and mitochondrial loci, suggesting introduction and
100 spread of a single clonal strain (Henricot et al., 2017). The extent of juniper decline varies,
101 with some populations showing wholesale dieback of bushes compared to others with only
102 localised patches of symptoms, suggesting populations have been infected at different times
103 and/or different site conditions promote different rates of spread.
104
105 Although interceptions of infected cypress and juniper trees in Scotland, England and
106 Germany confirm that infected material is being traded (Green et al., 2015; Werres et al.,
107 2014) the outbreak in British juniper populations in the wider environment remains the only
108 detected infection of a natural host population outside Argentina (Green et al., 2012). Globally,
109 juniper has a large, circumboreal distribution extending across the northern hemisphere but
110 as no investigation of environmental drivers of infection has been undertaken, the proportion
111 of juniper vulnerable to *P. austrocedri* infection is unclear.
112
113 In the UK, juniper has a wide but discontinuous distribution occupying much of Scotland and
114 northern England and remaining as scattered populations in southern England, Wales and
115 Northern Ireland (Fig. 1). Populations are undergoing long term declines in most areas as a
116 result of burning, afforestation, over-grazing, under-grazing, increased levels of diffuse
117 pollution (particularly nitrogen) and poor germination following warmer winter temperatures
118 (Broome and Holl, 2017; Clifton et al., 1997; Long and Williams, 2007; Sullivan, 2003;
119 Verheyen et al., 2009; Walker et al., 2017; Ward and Shellswell, 2017). It is difficult to estimate
120 the area of juniper lost specifically to disease but infected populations are widespread across
121 Scotland and England, where juniper occupancy of 10 x 10 km cells reportedly declined by 23
122 % and 44 % respectively between 2000 and 2016 (Plantlife, 2015).
123

The societal and environmental value of woodlands was recognised in the 2014 Tree Health Management Plan for England as several times higher than the commercial value of forestry (Department for Environment Food & Rural Affairs, 2014a) and the Scottish Plant Health strategy identifies plant health in the natural environment as integral to the £1.8 billion rural economy (The Scottish Government, 2016). Loss of UK juniper populations to *P. austrocedri* could be significant as the species is highly ecologically important as a dominant component of many habitats including woodland, scrub, heath, dune and calcareous grassland, as a nurse species ameliorating environmental conditions and protecting other seedlings from herbivory, a rare source of winter food and nesting habitat for birds, and a host of many specialist fungi and insects (Thomas et al., 2007a; Ward and Shellswell, 2017; Wilkins and Duckworth, 2011).

As juniper occupies such a broad variety of habitats, trees are subject to different environmental conditions and land uses that may alter their susceptibility to disease. Epidemics occur across a range of spatial scales, arising first as microscopic infections that can spread to whole plants, populations and landscapes (Gilligan and Van Den Bosch, 2008). Successful disease control requires matching of the scale of management to the inherent scale of spread as mediated by host population connectivity and pathogen dispersal distances (Cunniffe et al., 2016). Transmission of soil borne pathogens is likely to occur across short distances resulting in highly aggregated infection prevalence and spatially variable exposure to pathogens within host populations (Penczykowski et al., 2018). However, very few studies of soil borne Phytophthoras investigate spread at field scale and those that do use small (< 20) sample sizes (La Manna and Matteucci, 2012; La Manna and Rajchenberg, 2004a; Nagle et al., 2010; Tippett et al., 1989).

We measured juniper symptoms in 147 quadrats across three, geographically separate juniper populations with contrasting infection intensities and analysed the data using Generalised Linear Mixed Models (GLMMs) to compare drivers of spatial variation in symptoms at field scale. Correlative approaches, such as GLMMs, are appropriate tools to perform such

exploratory analyses as they can accommodate a broad range of potential covariates as is necessary when drivers of pathogen dispersal and spread in the invaded range are poorly understood (Purse and Rogers, 2009).

We expected *P. austrocedri* infection of juniper would exhibit similar responses to environmental covariates as infected Chilean cedar, which occupies a similarly diverse range of ecotypes. Population level studies in Argentina found area of foliage symptoms increased in microsites situated at low altitude with poor soil drainage, flat slopes, close proximity to watercourses and fine soil textures, with greater infection of female cedars because they typically occupy wetter microsites (Baccalá et al., 1998; V. a El Mujtar et al., 2012; La Manna et al., 2008; L. La Manna and Rajchenberg, 2004; Ludmila La Manna and Rajchenberg, 2004). In addition, we expected that the area of symptoms in juniper would increase with i) increasing host density, as inoculum production is likely to increase with availability of host tissue and dispersal distances between roots will be reduced (Anderson and May, 1986; Dillon et al., 2014); ii) increased ungulate herbivory, and proximity to deer and sheep tracks and lie-ups, as evidence for increased exposure to inoculum transported in soil on herbivore hooves (Jules et al., 2002; La Manna et al., 2013); and iii) increasing area of individual vascular plant taxa in the associated community that indicate conducive soil conditions for *P. austrocedri*. Given the contrast in abiotic and biotic conditions occupied by each population, we further expected that the relative importance of the investigated covariates would vary between locations and require site specific strategies to manage individual juniper populations.

2.0 Methods

2.1 Study Areas

Three infected juniper populations from where *P. austrocedri* had previously been isolated (Henricot et al., 2017) were selected to best represent the diversity of climatic, topographic and edaphic conditions occupied by juniper. Two populations are located in Scotland: one in Perthshire (P) and one in the Cairngorms (C), and one population is situated in the Lake District (LD) in the north of England. In all three locations, the juniper population is a component feature of a Special Area of Conservation designated habitat and a qualifying interest of a Site of Special Scientific Interest (SSSI; Fig. 1).

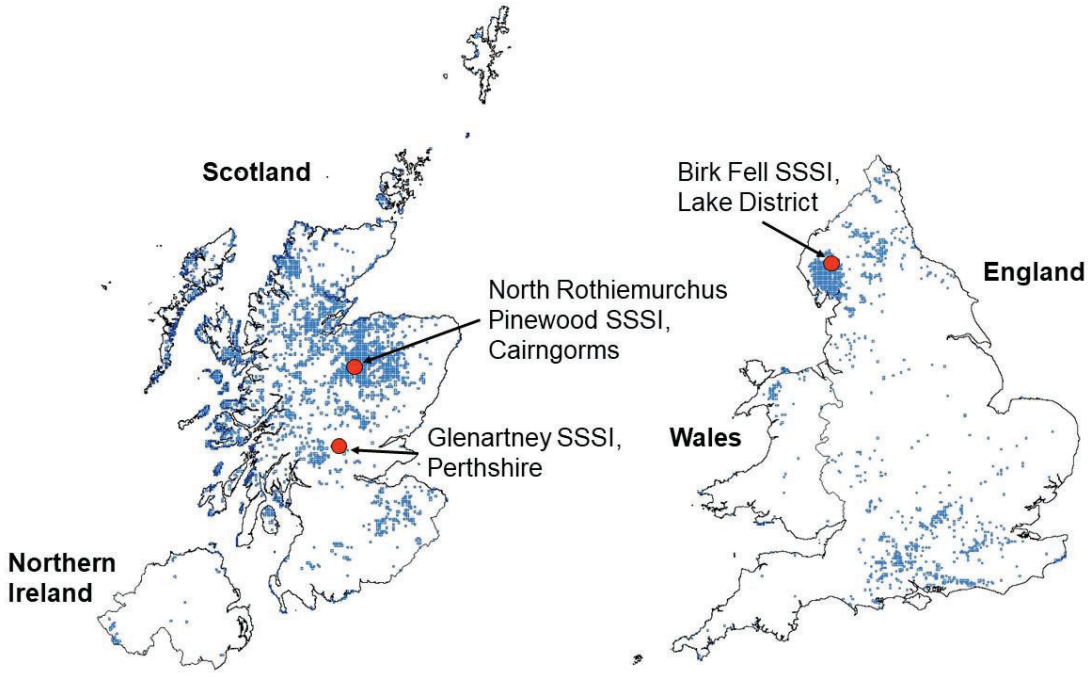

Figure 1. SSSI name and location of the three juniper study populations mapped against the distribution of UK juniper (*Juniperus communis* s. l.) at 2 x 2 km resolution (shown in blue) recorded during the period 2000 – 2017 (Botanical Society of Britain and Ireland, 2017).

Each population contained 100 – 130 hectares of continuous juniper cover. The greatest area of mortality was observed in the Perthshire population; symptoms were first reported in 2004 and represented a 20% decline in area of live juniper trees compared to a 1983 baseline survey (Tene et al., 2007). The precise duration of infection in the Lake District and Cairngorms populations is unknown, but *P. austrocedri* symptoms were first noted after 2010, and a lower proportion of symptomatic juniper was observed at both sites potentially consistent with a more recent introduction.

2.2 Quadrat stratification

Juniper was sampled using 10 x 10 m quadrats from pre-selected locations stratified according to the area and density of juniper, altitude, slope and distance to watercourses. A 2010 distribution map of the Perthshire juniper population derived from 15 cm full colour (RGB) and false colour infrared (CIR) imagery was provided by Scottish Natural Heritage (Whittome, 2010) and distribution maps of the remaining two populations were classified from 25 cm RGB imagery supplied for 2010 by NeXTPerspectives™. The classification methods are described in Appendix A.

To capture differences in juniper abundance and density, the area of juniper predicted by the image classifications was measured in 10 x 10 grid cells using landscape class statistical functions in the SDMTools package (Van der Wal et al., 2014) implemented in R v. 3.4.2 (R Core Team, 2017). To understand if each 10 x 10 m cell was isolated from other juniper stands or part of a larger stand, the area of juniper in 30 x 30 m including each 10 x 10 m grid cell was also calculated, producing distributions of juniper % cover at each scale for each study population (Fig. 2). These distributions were used to devise eight categories to describe juniper abundance that could be easily identified in the field. Each 10 x 10 m cell containing juniper was assigned to one of four categories describing juniper % cover in 10 x 10 m (≤ 10, 11-25, 26-50, > 51 %) and to one of two categories characterising the area of juniper

surrounding the 10 x 10 m cell as isolated from (< 20 %), or contiguous with (> 21 %), juniper growing in the wider 30 x 30 m.

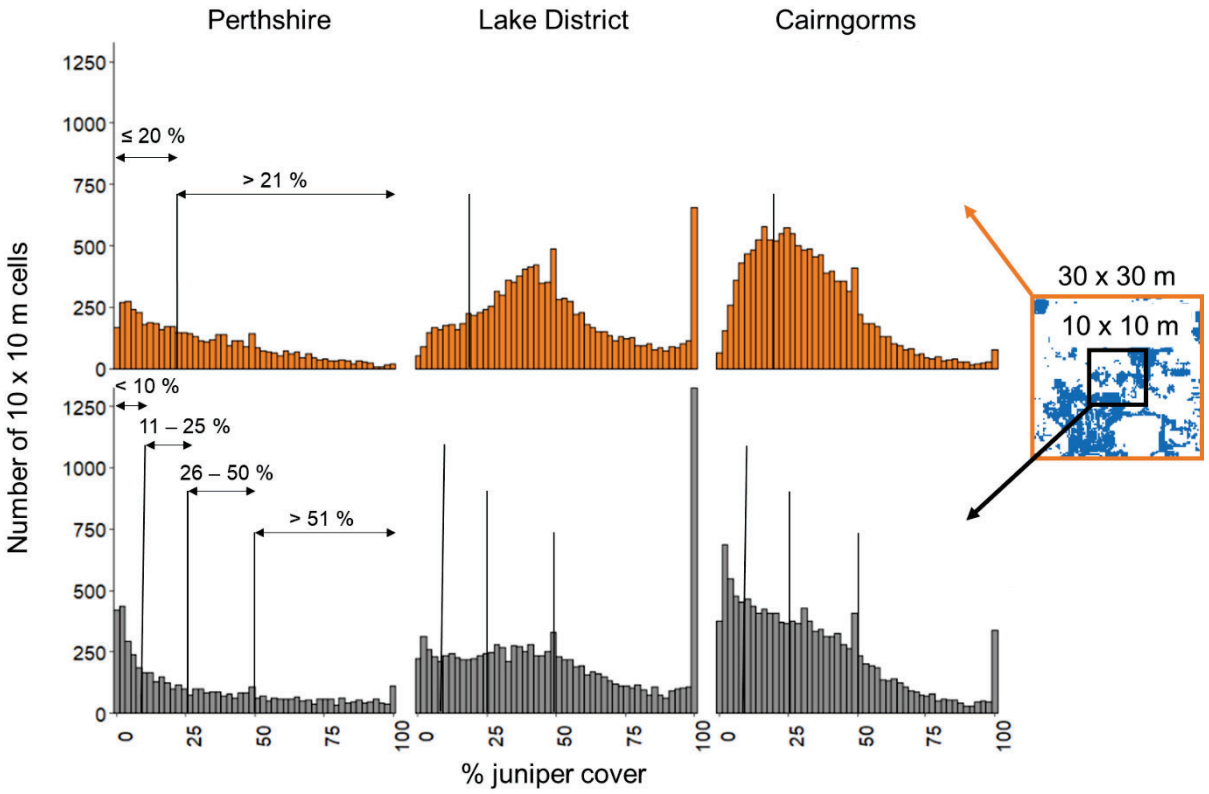

Figure 2. Number of 10 x 10 m cells per study population with estimated % cover of juniper (shown in blue) across 10 x 10 m (grey) cells and the surrounding 30 x 30 m (orange). Thresholds used to divide juniper % cover into categories at each scale are marked with black lines.

Layers of slope and aspect were calculated from the resampled NeXTPerspectives™ 10 m DEM using the *terrain* function in the raster package (Hijmans, 2016). Slope, aspect and altitude were then extracted to the centroid of each 10 x 10 m grid cell containing juniper. Euclidean distance (m) from the nearest watercourse to each 10 m grid cell centroid was measured from a rasterised version of the 50 m digital rivers network (Moore et al., 2000).

Survey locations were identified by randomly selecting 10 x 10 m cells out of each category of juniper abundance, in proportion to the total number of cells present in each category, to add up to 50 selected cells per study population. This proportional sampling procedure was repeated five times per population. Each sample of fifty was plotted across the altitudinal, slope and watercourse proximity gradients occupied by juniper at each location. The selection capturing the widest distribution of cells across each of the three gradients was chosen for survey.

2.3 Survey of spatial patterns in juniper symptoms

Quadrat sampling was carried out over five days at each location in October 2017. Quadrats were geo-located using ArcPad v. 10.2 on a Panasonic FZ-GI tablet with GPS accuracy to 3 m. To minimise transference of inoculum across populations, areas of high and low infection were visited on different days and all equipment breaking the soil surface (e.g. marker poles, soil moisture probes) was disinfected between quadrats. All other equipment was thoroughly disinfected between study populations.

Juniper quadrats were placed as close to pre-selected locations as was possible to meet the abundance criteria by estimating the area of juniper in 10 x 10 m and scoring abundance in 30 x 30 m as a binary measure of more or less than 20 %. The area of symptomatic juniper was measured as a fraction of the total area of juniper present in each quadrat, where symptoms constituted foliage discolouration and dead needles (retained or dropped) that extended to a minimum of a whole branch and did not result from either browsing or mechanical damage. Where a distinctive phloem lesion typical of *P. austrocedri* could be found, a 500 mg tissue sample was collected from one representative symptomatic tree per quadrat. The sampled tissue was stored at - 20 °C until quantitative real-time PCR (qPCR) could be carried out following the protocol described in Mulholland et al. (2013) to verify the consistent presence of *P. austrocedri* across each population.

261

262 **2.4 Abiotic and biotic predictors**

263

264 We measured a suite of potential abiotic and biotic predictors of spatial patterns in
265 *P. austrocedri* symptoms and included these in statistical models for each population (Table
266 1). The following predictors were measured in each field quadrat.

267

268 The binary observation of ≤ 20 % or > 21 % juniper cover across 30 x 30 m to distinguish
269 between quadrats situated in isolated or contiguous juniper stands was included in the model
270 as juniper "density". The area of juniper bearing berries was used to estimate the area of
271 female juniper. Area of herbivore damage was measured as the area of bark stripping plus
272 any resulting dead branches / stems (i.e. mechanical breakage from wind or snow damage
273 was excluded). This metric was not included in Cairngorm models as herbivory was only
274 detected in nine quadrats, encompassing an area greater than 10 cm^2 in only three quadrats.

275

276 Soil moisture was measured as % volumetric water content (VWC) using a FieldScout TDR
277 300 probe. Shallow soil and surface rock only permitted measurements using the 3.8 cm depth
278 setting across the Lake District population, whereas measurements were collected at 20 cm
279 depth in Perthshire and the Cairngorms. Measurements were collected from: i) areas within
280 each quadrat where juniper was absent; ii) under asymptomatic juniper; and iii) under
281 symptomatic juniper. An equal number of measurements (minimum four) were collected from
282 each category present, resulting in eight to twelve point sample measurements from which
283 mean soil moisture was calculated (% VWC).

284

285 Area of vascular plant taxa present in each quadrat was recorded according to a target list
286 (Appendix B) of taxa likely to co-occur with juniper in the study population habitats, that
287 indicate placement of microsites along soil moisture, nitrogen and pH gradients. Use of
288 individual target taxa allowed us to better distinguish between potential drivers of

289 *P. austrocedri* symptom severity and find a small number of common, easily identifiable
290 indicator taxa that land managers could use to predict microsites at higher or lower risk of
291 infection.
292
293 Mapping in the field was carried out using the tracking function in ARCpad, to record any
294 watercourses additional to the 50 m digital rivers network (Moore et al., 2000). These were
295 merged with the original dataset and used to recalculate the watercourse proximity (m) metric
296 for each quadrat. Clearly visible deer and sheep tracks were also mapped and proximity to
297 sampled quadrat centroids measured as an alternative way to measure the risk of inoculum
298 transference to juniper from herbivores, but stocking density and ground condition only
299 permitted collection of a reliable dataset from Perthshire.
300

Table 1. List of covariates included in full subset model selection for each population (P = Perthshire, LD = Lake District, C = Cairngorms). Number of sampled quadrats: P = 51, LD = 46, C = 50.

Measurement category	Specific measurement	Population		
		P	LD	C
Juniper density 30 x 30 m quadrat	≤ 20 % or > 21 % juniper cover	x	x	x
Juniper metrics 10 x 10 m quadrat	Area of juniper bearing berries (m^2)	x	x	x
	Area of herbivore damage (m^2)	x	x	
Soil moisture	Mean of point samples across quadrat (% VWC)	x	x	x
Vascular plant indicators	Area of individual target taxa (m^2)	x	x	x
Watercourse proximity	Euclidean distance from quadrat centroid to nearest mapped river (m)	x	x	x
Grazing activity	Distance from quadrat centroid to nearest deer or sheep track (m)	x		
Topographic metrics extracted to 10 x 10 m quadrat centroid	Altitude (m)	x	x	x
	Slope (°)	x	x	x
	Aspect (°)			x
Soil type (250 m resolution) extracted to 10 x 10 m quadrat centroid	**Perthshire:**			
	Brown forest Balrownie	x		
	Brown forest Gourdie	x		
	Organic soil, peaty gleys	x		
	Non-calcareous gleys	x		
	Peaty gleys Balrownie	x		
	Cairngorms:			
	Humus-iron podzols; some brown forest soils, noncalcareous gleys and peaty gleys			x
	Humus-iron podzols; some peaty gleys and humic gleys			x
Habitat (NVC community)	**Perthshire:**			
	W19 *Juniperus communis* woodland	x		
	Acid grasslands (U4, U20, U24)	x		
	Mires (M10, M23)	x		
	Mosaic (U5, M15)	x		
	Cairngorms:			
	H12 *Calluna vulgaris* – *Vaccinium myrtillus* heath			x
	W18 Scots pine woodland with heather			x
	U4 *Festuca ovina - Agrostis capillaris - Galium saxatile* grassland			x
	Coniferous plantation			x

306 The remaining covariates were obtained from existing GIS datasets. Altitude, slope and aspect
307 were extracted to each quadrat centroid from the resampled NeXTPerspectives™ 10 m layers
308 prepared for the plot stratification. Aspect was not included in the Perthshire or Lake District
309 models as more than 60 % of quadrats at each location were clustered in the same octant.
310
311 The soil type underlying each quadrat centroid was extracted from 250 m resolution datasets,
312 obtained from a digitised version of the soil map produced by Forbes (1984), the Soilscapes
313 dataset (Farewell et al., 2011) and the National Soil Map of Scotland (James Hutton Institute,
314 2011) for the Perthshire, Lake District and Cairngorms populations respectively. Soil type was
315 omitted from model selection for the Lake District population as at 250 m resolution all of the
316 quadrats were placed in “freely draining acid loamy soils over rock” (Farewell et al., 2011).
317
318 To test if a broader description of the vegetative community is a better predictor of
319 *P. austrocedri* symptoms, because it captures more information about edaphic conditions than
320 the presence of individual taxa, National Vegetation Classification (NVC) community data,
321 supplied by Scottish Natural Heritage (2017), was included as a covariate for the Perthshire
322 and Cairngorms populations (Table 1). The eight Perthshire communities were simplified to
323 these four broad types (Table 1), amalgamated as follows: acid grasslands (U4 *Festuca ovina*
324 - *Agrostis capillaris* - *Galium saxatile*; U20 *Pteridium aquilinum* - *Galium saxatile*; U24
325 *Arrhenatherum elatius* - *Geranium robertianum*), mires (M10 *Carex dioica* – *Pinguicula*
326 *vulgaris*; M23 *Juncus effusus/acutiflorus* – *Galium palustre*) and mosaic communities
327 suggesting transition from drier to wetter soil (U5 *Nardus stricta* – *Galium saxatile*; M15
328 *Trichophorum germanicum* - *Erica tetralix* wet heath) (Rodwell, 1991). No NVC data was
329 released for the Lake District population.
330
331
332
333

334 **2.5 Model specification**

335

336 To investigate the relationships between the area of *P. austrocedri* symptoms and
337 environmental covariates, we used a Bayesian beta-binomial Generalised Linear Mixed Model
338 (GLMM) fitted using the Integrated Nested Laplace Approximation (INLA) method with the R-
339 INLA package (Rue et al., 2009) implemented in R v. 3.4.2 (R Core Team, 2017). Models
340 were fitted to the number of square metres of symptomatic juniper in each 10 x 10 m quadrat.
341 Using the beta-binomial distribution enabled us to take account of the area of juniper in each
342 cell while allowing the probability of infection to have extra variation associated with spatial
343 clustering of symptoms (overdispersion), thereby accounting for the high frequency of
344 quadrats that contain wholly asymptomatic or symptomatic juniper (Hughes and Madden,
345 1993).

346

347 In particular, our model used the q = 12 environmental covariates for the i^{th} location
348 $\{x_{j,i} | 1 \leq j \leq 16\}$ to estimate the mean probability of infection via a logit link function

349

350 $$\text{logit}(\mu_i) = \beta_0 + \beta_1 x_{1,i} + \cdots + \beta_q x_{16,i},$$

351 in which β_0 is an intercept and β_j is the regression coefficient for the j^{th} predictor. This estimate
352 of the mean probability is then used to predict the area of symptomatic juniper in the i^{th} location
353 (η_i) via

354 $$\eta_i \sim \text{beta-binomial}(\mu_i, \gamma, N_i),$$

355

356 in which N_i is the total area of juniper in the i^{th} cell (m^2) and γ is the overdispersion parameter
357 of the beta-binomial distribution (that was assumed to be constant across all cells at each
358 site). In our Bayesian estimation procedure all regression parameters, including the intercept,
359 were assumed to have minimally informative priors of the form

360

$$\beta_q \sim \text{Normal}(0, 1/0.001).$$

2.6 Model selection

All covariates were centred and standardized prior to model fitting and no pairs of covariates used in any models were correlated with a Pearson r^2 value ≥ 0.6 (Appendix D). Models were run in two stages. We first performed a full subset selection using all possible combinations of covariates marked against each population (Table 1) except the vascular plant indicators, producing 1023 models for both Perthshire and the Cairngorms, and 127 models for the Lake District, which had seven as opposed to ten covariates. Model fit was compared using the Deviance Information Criterion (DIC), a Bayesian generalisation of the Akaike Information Criterion (AIC) derived as the mean deviance adjusted for the estimated number of parameters in the model to provide a measure of out-of-sample predictive error (Gelman and Hill, 2006). The model with the lowest DIC is the model with the most support in the data, but the set of models with DICs within two units of the top model DIC are considered to have equivalent support in the data and formed the "top model set". The area of each vascular plant indicator, present in ten or more quadrats at each population, were then added to the formulae for the top model set per population to assess (using DIC) if the addition of any one indicator improved model fit. Nine additional models were run for Perthshire and the Lake District, and ten for the Cairngorms (Table 3).

To assess the importance of covariate effects, we summarised marginal posterior distributions using 95 % (0.025 and 0.975 quantiles of the posterior distribution) Bayesian credible intervals (BCI). The relationship between each covariate and the area of symptoms is considered strongest where BCI do not bridge zero, very strong when ≥ 0.95, strong when ≥ 0.90 – 0.94, and weak when ≥ 0.80 – 0.89 of the BCI are above or below zero. Where a strong or very strong relationship was found between the area of symptoms and a covariate, we report the

388 percentage of the posterior predicted data that overlaps zero as calculated in R v. 3.5.2 (R
389 Core Team, 2018) using the *rollmean* function in the zoo package (Zeileis and Grothendieck,
390 2005). The explanatory power (goodness of fit) of each model was evaluated using root mean-
391 square error (RMSE) calculated between the predicted posterior mean values and the
392 corresponding mean sampled area of symptomatic juniper. The residuals of the top models
393 were checked for spatial autocorrelation using Moran's I statistic implemented using the
394 *correlog* function in R package ncf v 1.2.8 (Bjornstad, 2019). Pairs of plots were divided into
395 different distance bins at 100 m intervals between 0 and the maximum distance between plot
396 pairs for each site and the Moran's I value was then calculated for each distance bin. One
397 hundred paired distances were randomly resampled per distance bin to assess Moran's I
398 correlation significance (Appendix D). As no spatial autocorrelation was found in the residuals,
399 the addition of a spatial component (mesh) to the model formulation was not required.
400
401

3.0 Results

3.1 Prevalence of symptoms of *P. austrocedri* infection

Fifty-five percent of juniper surveyed in the Perthshire population showed symptoms compared to 28 % in the Lake District and 23 % in the Cairngorms populations, consistent with a possible earlier pathogen introduction in Perthshire (Fig. 3). Though quadrats containing no symptomatic juniper were found in all three populations, the mean area of symptomatic juniper found in Perthshire quadrats was 19 ± 20 m^2 out of a mean 34 ± 28 m^2 area of juniper, compared to a mean of 7 ± 11 m^2 of symptomatic juniper in quadrats from the Cairngorms population where the mean juniper cover found per quadrat was similar (33 ± 22 m^2). The mean area of juniper in the Lake District quadrats was higher (44 ± 27 m^2) with an intermediate mean area of symptomatic juniper (13 ± 18 m^2). Because detection of symptomatic lesions is limited to above-ground live tissue, qPCR results are less reliable indicators of infection than symptoms. However, positive qPCR results were obtained across the full extent of each population giving confidence that site-wide observations of symptoms result from *P. austrocedri* infection (Appendix C).

The mean, standard deviation and range of covariates measured and tested in models across all three populations is shown in Table 2. The Perthshire population is characterised by fragmented juniper stands, only 35 % of quadrats contained more than 21 % juniper cover across 30 x 30 m compared to c. 70 % in the Lake District and Cairngorm populations where juniper grows in denser stands (Fig. 3, Table 2). Perthshire population quadrats were never further than 174 m from a river or drain, compared to 840 and 820 m in the Lake District and Cairngorms populations respectively (Fig. 3, Table 2). The Lake District population occupied the largest range of altitude (234 m compared to 132 m in Perthshire and 78 m in the Cairngorms) with up to 45° slopes compared to just 20° in both Scottish populations (Fig. 3; Table 2). The Cairngorms population had the driest soil conditions across the quadrats (Table

2) with mean soil moisture of 33 % VWC, which is 27 % and 48 % drier than the mean soil moisture found across Lake District and Perthshire quadrats respectively.

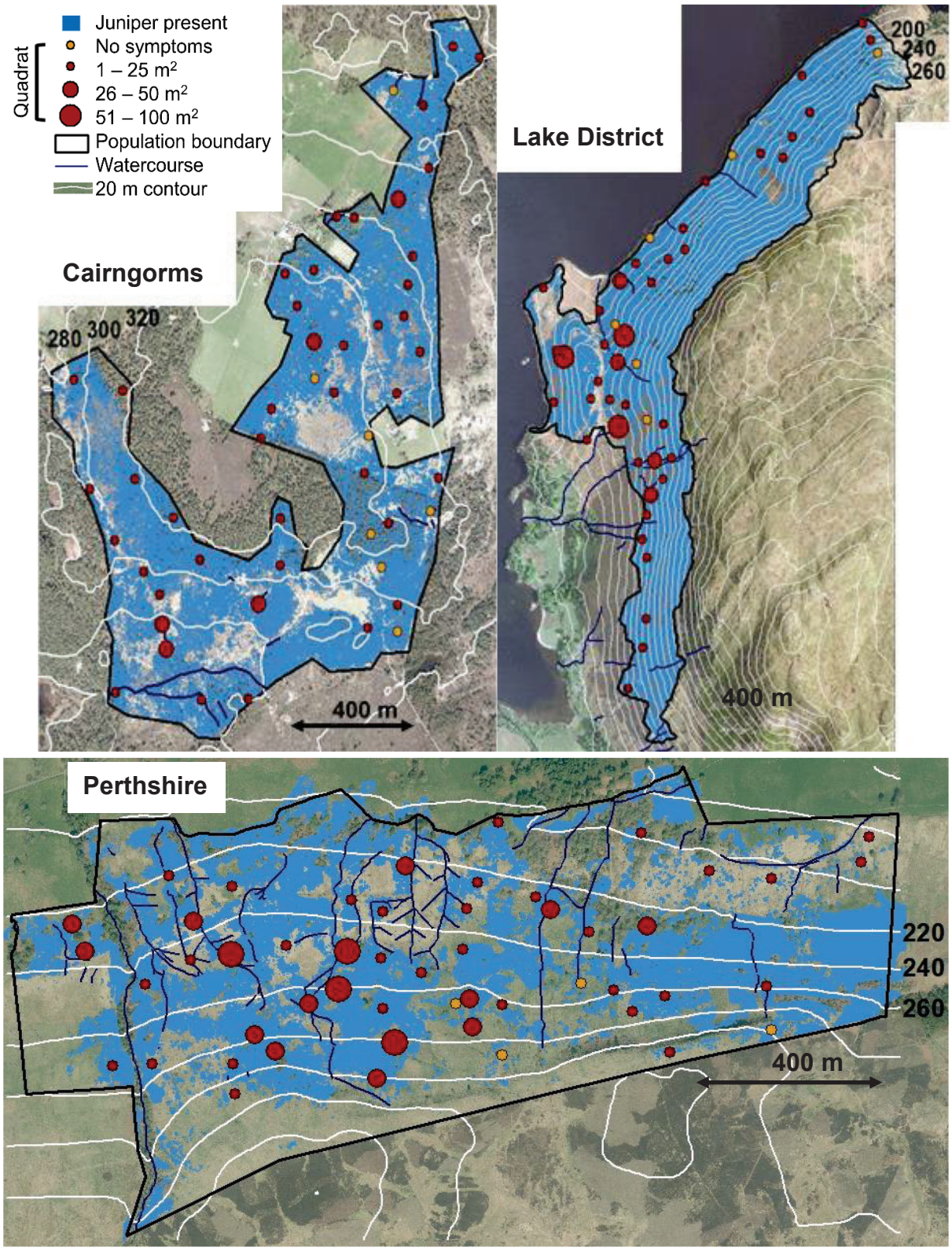

457 **Figure 3.** Map of surveyed juniper populations showing the distribution of juniper in relation
458 to the watercourse, altitude and slope covariates used to stratify sampling. The distribution
459 of samples, collected in 10 x 10 m quadrats, is shown with circles coloured orange where no
460 *P. austrocedri* symptoms were found and red where symptoms were present. Circle size
461 corresponds to categories representing the area of symptoms estimated in each quadrat.
462 Imagery licensed to UK Centre for Ecology & Hydrology for PGA through Next
463 Perspectives™
464

Table 2. Comparison of surveyed juniper population covariate means ± 1 s.d., and ranges, measured from 10 x 10 m quadrats. P = Perthshire, LD = Lake District and C = Cairngorms study populations. Only numerical / binary coded variables included in the first stage of GLMM modelling (i.e. excluding species indicators) are displayed. Covariates not included in models for specific populations are greyed out.

Covariate	Mean ± s.d.per quadrat			Range per quadrat		
	P	LD	C	P	LD	C
Area of symptomatic juniper (m^2)	19 ± 20	13 ± 18	7 ± 11	0 - 79	0 - 70	0 - 45
Area of juniper (m^2)	34 ± 28	44 ± 27	33 ± 22	2 - 99	1 - 90	1 - 80
Juniper density (% quadrats nested in 30 x 30 m with > 21 % juniper cover)	35	72	70	NA	NA	NA
Area of juniper bearing berries (m^2)	10 ± 12	9 ± 15	4 ± 9	0 - 49	0 - 66	0 - 49
Area of herbivore damage (m^2)	2 ± 8	0 ± 1	0 ± 1	0 - 50	0 - 3	0 - 7
Mean soil moisture (% VWC)	45 ± 12	63 ± 17	33 ± 9	28 - 84	33 - 108	15 - 52
Watercourse proximity (m)	42 ± 37	144 ± 209	240 ± 193	1 - 174	0 - 840	2 – 820
Grazing activity (m)	16 ± 16	72 ± 68	31 ± 49	0 - 70	1 - 212	1 - 213
Altitude (m)	250 ± 30	248 ± 63	303 ± 21	182 - 314	150 - 384	256 - 334
Slope (°)	11 ± 4	32 ± 7	6 ± 4	5 - 23	15 - 45	1 – 20
Aspect (°)	158 ± 145	276 ± 53	174 ± 99	2 - 357	88 - 342	10 - 348

Nine vascular plant indicators were present in ten or more quadrats in the Perthshire population, nine in the Lake District and ten in the Cairngorms (Table 3). The mix of indicators recorded highlights the difference in microsites occupied by the juniper study populations (Table 3). Of 42 target indicators, only one, V*accinium myrtillus*, was present at all three study populations while quadrat frequency for the remaining indicators varied from 19 – 42 quadrats.

Indicators of drier, moderately fertile soils were only present in the Lake District quadrats, where no indicators of high soil moisture and three indicators of highly acidic, infertile microsites were also found. In contrast, there were two indicators of high soil moisture in the Cairngorms, six for highly acidic, infertile soils (four present in > 40 of 50 quadrats) and no indicators of drier, moderately fertile microsites (Table 3). Quadrats from Perthshire were dominated (both in terms of species composition and prevalence across quadrats) by seven taxa indicating moderate soil moisture (Table 3). However, although only one taxon (*Molinia caerulea*) indicating high soil moisture was recorded, it was found in 21 of the 51 quadrats, suggesting widespread, continuous waterlogging across the site.

Table 3. Number of 10 x 10 m quadrats containing vascular plant indicators (where present in ≥ 10 quadrats), out of the total number of quadrats (shown in brackets) surveyed across each population. P = Perthshire, LD = Lake District, C = Cairngorms juniper populations. Taxa were assigned to soil condition categories devised from Ellenberg values given in Hill, Preston, & Roy (2004). Two categories were used to describe reaction (R) and nitrogen (N) soil conditions: highly acidic (R=2) and low nitrogen (N = 1-2) or slightly acidic (R=3-5) and moderately fertile (N = 3-5). Taxa were then categorized according to soil moisture (F) as high (F = 8-9), moderate (F = 6-7) or lower (F = 5).

Taxon	Soil condition			Population		
	R	N	F	P (51)	LD (46)	C (50)
Vaccinium myrtillus	2	1-2	5	19	27	42
Calluna vulgaris	2	1-2	5		19	46
Pinus sylvestris	2	1-2	5			31
Vaccinium vitis-idaea	2	1-2	6-7			42
Erica cinerea	2	1-2	6-7		13	12
Erica tetralix	2	1-2	8-9			13
Dryopteris affinis	3-5	3-5	5	30	22	
Oreopteris limbosperma	3-5	3-5	5	22	10	
Dryopteris dilatata	3-5	3-5	5	31		
Juncus conglomeratus	3-5	3-5	5	19		10
Juncus effusus	3-5	3-5	5	14		12
Deschampsia cespitosa	3-5	3-5	5	24		
Rubus fruticosus agg.	3-5	3-5	5	12	12	
Pteridium aquilinum	3-5	3-5	6-7		45	
Betula pendula	3-5	3-5	6-7		15	15
Ilex aquifolium	3-5	3-5	6-7		10	
Molinia caerulea	3-5	3-5	8-9	21		15

3.2 Abiotic and biotic drivers of spatial variability in disease symptoms of *P. austrocedri*

The full subset selection modelling resulted in one top model each containing abiotic and biotic covariates for the Perthshire and Lake District populations, and two models for the Cairngorms population (Table 4). All models included a strong relationship between increasing area of *P. austrocedri* symptoms and a measure of increasing soil moisture (Table 5). When the area

of different vascular plant indicators was added to these models, this resulted in one top model with improved fit for each population, with strong, positive relationships between increasing symptoms and increasing soil moisture still included but additionally identifying taxa that aid identification of microsites vulnerable to *P. austrocedri* infection in different habitats (Table 4). Across all sites, models with abiotic and biotic covariates vastly outperformed the null model with no covariates.

Table 4. Model results (DIC, RMSE, dispersion and list of covariates present) for each surveyed population, comparing the null model with the top set of models produced before and after addition of vascular plant indicators.

Juniper population	Model	DIC	RMSE	Dispersion	Covariates
Perthshire	Without indicators	167.45	43.89	0.48	Juniper density, berry-bearing, herbivore damage, soil moisture, watercourse proximity, grazing activity, altitude, slope, soil type, habitat
	With indicators	134.96	42.59	0.45	As above with area of *Dryopteris dilatata*
	Null	301.98	37.04	0.55	N/A
Lake District	Without indicators	264.64	32.64	0.44	Juniper density, berry-bearing, soil moisture, watercourse proximity, altitude, slope
	With indicators	208.84	22.99	0.42	As above with area of *Rubus fruticosus* agg.
	Null	301.77	41.54	0.57	N/A
Cairngorms	Without indicators	226.71	21.22	0.33	Juniper density, berry-bearing, soil moisture, aspect, soil type, habitat
		225.40	21.38	0.33	Juniper density, berry-bearing, soil moisture, slope, aspect, soil type, habitat
	With indicators	191.92	21.09	0.30	As above with area of *Erica tetralix*
	Null	293.63	43.92	0.58	N/A

The Cairngorms population models all predicted the distribution of symptoms with reasonable accuracy, as the predicted area of symptoms was within 20 % of observed values (Table 4). Addition of a plant indicator improved symptom prediction by 10 % in the Lake District to within 20 % of the observed values. However, predictive model performance was poorer for the Perthshire population where the predicted area of symptomatic juniper was only within 40 %

518 of observed values from both the full subsets and plant indicator models (Table 4). No
519 evidence of overdispersion was found in the residuals of any of the top models (Table 4).
520
521 The top model produced for the Perthshire population from the full subset selection included
522 all ten possible covariates (DIC 167.45) with only one strong relationship identified between
523 increasing area of symptomatic juniper and increasing soil moisture (Table 5, BCI = 0.70,
524 4.08). Model fit improved by 32 units (DIC 134.96) when area of *Dryopteris dilatata* was
525 included: a species of large fern that prefers moist, moderately acidic and fertile soils (Table
526 3). In this model, the strongest effect (BCI did not bridge zero) was increasing area of
527 *P. austrocedri* symptoms with increasing area of *D. dilatata* (BCI = 0.70, 4.08). The area of
528 symptoms also increased very strongly with increasing soil moisture (BCI = -0.04, 1.20) and
529 decreasing altitude (BCI = -1.72, 0.05), and strongly with decreasing area of herbivore damage
530 (BCI = -1.41, 0.05).
531
532 Six of the seven potential covariates collected across the Lake District population were
533 included in the top model prior to adding indicators (DIC 264.64) with area of *P. austrocedri*
534 symptoms again showing a strong response to soil moisture related covariates, with
535 symptoms strongly increasing with decreasing distance to watercourses (Table 6, BCI = -0.99,
536 0.08). Including brambles, *Rubus fruticosus* agg., improved the model fit by 56 DIC units
537 (Table 4). The BCI for the relationship between increasing area of symptoms and decreasing
538 distance to watercourses did not bridge zero (BCI = -1.26, -0.14) and the area of symptoms
539 strongly increased with decreasing area of *R. fruticosus* agg. (BCI = -4.19, 0.09), recorded in
540 12 of 46 quadrats (Table 3).
541
542 Two top models were found for the Cairngorms population including six, and seven, of nine
543 possible covariates; including slope marginally improved model fit (DIC decreased from
544 226.71 to 225.40). In both models the BCI for soil moisture did not bridge zero, showing a very
545 strong relationship between increasing area of *P. austrocedri* symptoms with increasing soil

546 moisture (Table 7). When indicator taxa were added, only one top model (including slope) was
547 found. Of the ten indicator taxa explored, the top model contained area of cross-leaved heath
548 (*Erica tetralix*). Model fit was improved by 35 and 33 DIC units compared to the full subset
549 selection models (Table 4). Increasing area of symptoms with increasing area of *E. tetralix*
550 was the only strong relationship present, for which the BCI did not bridge zero (BCI = 0.26,
551 1.28). Recorded in 13 of 50 quadrats (Table 3), *E. tetralix* is the only indicator found out of the
552 target list for highly acidic, infertile microsites with high soil moisture.
553
554 In addition to soil moisture directly measured within quadrats, top models for all populations
555 contained weak effects of juniper density and area of juniper bearing berries, and weak effects
556 of slope on symptoms, despite differences in the range of variation sampled across each
557 population (Table 2). Evidence for the direction of correlations between area of symptoms and
558 juniper density and area of juniper bearing berries varied across the three populations, being
559 consistently positive in the Perthshire population (Table 5), but with less clear directional
560 effects in the other two populations (Tables 6 & 7). Directional effects for slope were also less
561 clear and were generally weaker than those identified for juniper covariates (Tables 5, 6 & 7),
562 Soil and habitat (NVC community) types only included in the Perthshire and Cairngorms
563 models were also always present. However, none of these covariates showed strong
564 relationships with increasing area of symptoms but removing them resulted in poorer model
565 fit (i.e. the DIC increased by more than two units). This suggests these covariates are playing
566 a role in the extent of symptoms in the different populations but the precise nature of these
567 relationships remains unclear.
568
569

570 **Table 5.** Posterior estimates (mean, standard deviation (SD), 2.5 % and 97.5 % quantiles, and % that does
571 not bridge zero) for fixed effects included in the top model set for the Perthshire juniper population.

	Covariate	Mean	SD	2.5%	97.5%	% does not bridge zero
	Without indicator species (DIC = 167.45)					
	Soil moisture	0.59	0.31	0.01	1.21	100.00
	Altitude	-0.69	0.43	-1.57	0.13	92.71
	Herbivore damage	-0.39	0.29	-1.01	0.14	90.20
	Juniper density	0.29	0.25	-0.20	0.77	87.70
	Intercept	0.05	21.22	-41.61	41.67	50.17
	Berry-bearing	0.21	0.25	-0.27	0.70	80.19
	Grazing activity	-0.17	0.26	-0.67	0.34	75.21
	Watercourse proximity	-0.03	0.31	-0.66	0.55	53.17
	Slope	-0.08	0.39	-0.84	0.68	57.69
Habitat	Mosaic	-0.70	15.82	-31.76	30.32	51.17
	Mires	-0.03	15.82	-31.09	31.01	50.17
	Juniper wood	0.80	15.83	-30.28	31.86	52.17
	Acidic grassland	-0.08	15.82	-31.14	30.96	50.17
Soil	Peaty gleys	0.22	14.15	-27.57	27.99	50.17
	Organic peaty gleys	0.37	14.15	-27.42	28.13	51.17
	Non-calcareous gleys	-2.65	14.19	-30.52	25.19	55.18
	Brown forest Balrownie	0.66	14.15	-27.13	28.43	51.17
	Brown forest Gourdie	1.40	14.16	-26.40	29.18	53.17
	With indicator species (DIC = 134.96)					
	Dryopteris dilatata	2.36	0.86	0.70	4.08	100.00
	Soil moisture	0.57	0.32	-0.04	1.20	95.21
	Altitude	-0.81	0.45	-1.72	0.05	95.19
	Herbivore damage	-0.65	0.37	-1.41	0.05	95.20
	Juniper density	0.25	0.52	-0.78	1.26	67.69
	Intercept	0.18	21.22	-41.48	41.81	50.17
	Berry-bearing	0.06	0.26	-0.45	0.57	57.68
	Grazing activity	-0.19	0.26	-0.70	0.33	75.21
	Watercourse proximity	-0.18	0.33	-0.85	0.45	67.70
	Slope	0.07	0.41	-0.73	0.87	55.18
Habitat	Mosaic	-0.97	15.82	-32.03	30.06	52.18
	Mires	-0.18	15.82	-31.24	30.86	50.17
	Juniper wood	1.45	15.84	-29.65	32.52	53.17
	Acidic grassland	-0.30	15.82	-31.37	30.73	50.17
Soil	Peaty gleys	-0.14	14.15	-27.93	27.63	50.17
	Organic peaty gleys	0.50	14.15	-27.29	28.26	51.17
	Non-calcareous gleys	-3.05	14.19	-30.91	24.80	57.68
	Brown forest Balrownie	1.06	14.16	-26.73	28.83	52.67
	Brown forest Gourdie	1.62	14.16	-26.18	29.41	54.17

572

573

574 **Table 6.** Posterior estimates (mean, standard deviation (SD), 2.5 % and 97.5 % quantiles, and % that does
575 not bridge zero) for fixed effects included in the top model set for the Lake District juniper population.

Covariate	Mean	SD	2.5%	97.5%	% does not bridge zero
Without indicator species (DIC = 264.64)					
Intercept	-1.28	0.45	-2.19	-0.43	100.00
Watercourse proximity	-0.41	0.27	-0.99	0.09	92.70
Soil moisture	0.09	0.25	-0.41	0.58	62.69
Juniper density	0.17	0.50	-0.78	1.17	62.67
Berry-bearing	0.00	0.22	-0.45	0.41	52.18
Altitude	0.22	0.24	-0.24	0.70	80.19
Slope	-0.26	0.28	-0.83	0.29	80.20
With indicator species (DIC = 208.84)					
Intercept	-1.29	0.43	-2.16	-0.47	100.00
Watercourse proximity	-0.66	0.29	-1.26	-0.14	100.00
Rubus fruticosus agg.	-1.81	1.09	-4.19	0.09	95.23
Soil moisture	0.00	0.25	-0.51	0.48	50.17
Juniper density	-0.21	0.55	-1.27	0.88	65.19
Berry-bearing	-0.04	0.22	-0.49	0.36	55.18
Altitude	-0.24	0.30	-0.82	0.35	77.68
Slope	0.06	0.29	-0.53	0.62	57.70

576

Table 7. Posterior estimates (mean, standard deviation (SD), 2.5 % and 97.5 % quantiles, and % that does not bridge zero) for fixed effects included in the top model set for the Cairngorms juniper population.

	Covariate	Mean	SD	2.5%	97.5%	% does not bridge zero
	Without indicator species (DIC = 226.71)					
	Soil moisture	0.54	0.22	0.09	0.98	100.00
	Berry-bearing	0.18	0.18	-0.18	0.53	82.68
	Intercept	-1.15	27.39	-54.93	52.58	51.17
	Juniper density	-0.18	0.44	-1.01	0.70	65.20
	Aspect	-0.02	0.21	-0.45	0.39	54.17
Habitat	Scots pine woodland	0.64	15.82	-30.43	31.67	51.17
	Heath	0.19	15.82	-30.86	31.22	50.17
	Coniferous plantation	-0.73	15.84	-31.83	30.34	51.17
	Acidic grassland	-0.09	15.82	-31.16	30.95	50.17
Soil	Humus-iron podzols; gleys	0.46	22.36	-43.44	44.33	50.17
	Humus-iron podzols; brown forest	-0.46	22.36	-44.37	43.40	50.17
	Without indicator species (DIC = 225.40)					
	Soil moisture	0.57	0.23	0.12	1.01	100.00
	Berry-bearing	0.17	0.18	-0.18	0.52	82.68
	Intercept	-1.08	27.39	-54.85	52.66	51.17
	Juniper density	-0.24	0.44	-1.09	0.65	70.19
	Slope	0.13	0.22	-0.31	0.54	72.69
	Aspect	-0.07	0.23	-0.52	0.37	60.17
Habitat	Scots pine woodland	0.67	15.82	-30.39	31.71	51.17
	Heath	0.17	15.82	-30.88	31.20	50.17
	Coniferous plantation	-0.76	15.84	-31.86	30.31	51.17
	Acidic grassland	-0.07	15.82	-31.14	30.97	50.17
Soil	Humus-iron podzols; gleys	0.52	22.36	-43.39	44.38	50.17
	Humus-iron podzols; brown forest	-0.52	22.36	-44.42	43.35	50.17
	With indicator species (DIC = 191.92)					
	Erica tetralix	0.73	0.26	0.26	1.28	100.00
	Soil moisture	0.19	0.27	-0.36	0.71	75.21
	Berry-bearing	0.15	0.18	-0.22	0.50	77.72
	Intercept	-1.72	27.39	-55.50	52.02	52.18
	Juniper density	-0.02	0.46	-0.88	0.91	52.68
	Slope	0.04	0.21	-0.39	0.45	57.70
	Aspect	0.05	0.23	-0.42	0.50	57.69
Habitat	Scots pine woodland	1.12	15.82	-29.95	32.16	52.67
	Heath	0.47	15.82	-30.59	31.50	51.17
	Coniferous plantation	-2.26	15.85	-33.39	28.84	55.18
	Acidic grassland	0.69	15.83	-30.39	31.73	51.17
Soil	Humus-iron podzols; gleys	0.30	22.36	-43.60	44.17	50.17
	Humus-iron podzols; brown forest	-0.30	22.36	-44.21	43.56	50.17

4.0 Discussion

Our study provides the first evidence from the northern hemisphere that, out of the wide range of potential abiotic and biotic drivers considered, and despite differences in the range of conditions, geographic location and infection intensity occupied by study populations, soil moisture is the best predictor of *P. austrocedri* symptom distribution in juniper at population scale. This is likely to result from the pathogen's dependence on soil moisture for zoospore dispersal (Green et al., 2015; Greslebin et al., 2007). We further showed that associated plant species with distinctive soil moisture requirements, such as cross-leaved heath, can be used to predict microsites at increased risk of infection. Results from the Lake District and Perthshire populations suggested that the pathogen may also be spread through movement of infected soil on herbivore hooves and tyre treads. Management actions accounting for pathogen transmission in both soil, and soil water are, therefore, needed to prevent or slow spread of *P. austrocedri*.

Introductions of non-native *Phytophthora* taxa have been reported from 176 countries across a wide range of climatic zones (Barwell et al., in review). Water availability is commonly identified as an important driver of terrestrial *Phytophthora* distributions at a range of scales. Globally, functional and species diversity increases with precipitation (Redondo et al., 2018). Landscape scale examples include increased incidence of *P. lateralis* in Port-Orford cedar with increasing creek drainage area (Jules et al., 2008), and increased *P. ramorum* infection of tanoak with increasing stream proximity (Peterson et al., 2014). In individual trees, the length of *P. cinnamomi* lesions increase in Jarrah with increasing precipitation (Bunny et al., 1995) because water is required to stimulate sporangial formation, trigger zoospore release and enable dispersal (Hardham, 2005).

The importance of soil moisture as a driver of *P. austrocedri* infection in juniper populations is likely to vary between sites with different soil types and hydrology. Area of symptoms

608 increased very strongly with point sampled soil moisture in both the Cairngorms and
609 Perthshire populations, which grow on deep soils formed from glacial till, with pockets of
610 gleying, that retain a high volume of soil moisture throughout the year. This is consistent with
611 population level studies of Chilean cedar where *P. austrocedri* infection increases with soil
612 waterlogging caused by high clay content (La Manna and Rajchenberg, 2004a) or features
613 restricting water permeability (La Manna & Rajchenberg, 2004b). Though microsite soil
614 moisture is partly a function of soil type, explicitly including soil type in the Cairngorms and
615 Perthshire models always improved model performance but never strongly predicted the area
616 of symptoms, probably because the available data for soil type were too coarse in spatial
617 resolution (250 m) to capture microsite variation. Spatial variation in area of symptoms was
618 also linked to soil moisture in the Lake District populations but here the strongest association
619 was between symptoms and decreasing proximity to watercourses rather than point sampled
620 soil moisture. Given the steep site topography and freely draining, shallow, sandy soil type, it
621 is likely that juniper in this population is only exposed to long term waterlogging where it grows
622 adjacent to watercourses. Stands of Chilean cedar growing in comparable (freely draining,
623 volcanic) soils also demonstrate increased infection with increasing proximity to watercourses
624 (Calı´, 1996; La Manna & Rajchenberg, 2004a).
625
626 A key challenge for investigating field scale drivers of disease is obtaining data at a suitably
627 detailed spatial resolution. Modelling microsite soil moisture patterns was prohibited by the
628 availability of fine scale data on hydrological processes (such as precipitation, potential
629 evaporation and runoff generation). Topographic wetness index (TWI), calculated from site
630 topography and watercourse networks, is commonly used as a proxy for soil moisture. In the
631 absence of variability in slope and altitude gradients, the calculation tends to overpredict
632 differences (Grabs et al., 2009) and did not yield an informative distribution map for the
633 Cairngorms juniper population (results not shown). It also assumes uniform soil properties and
634 does not account for complex bedrock surfaces, invalidating the data derived for the Lake
635 District population (results not shown) (Kopecký and Čížková, 2010). Measuring soil moisture

directly from stratified quadrats as % volumetric water content captured variation in water table heights but only represents conditions at a single point in time and differences between microsites may be exaggerated by rainfall events that occurred during the sampling period. We introduced the area of vascular plant indicators, selected to represent a range of soil moisture preferences, to test whether such indicators capture longer term water table levels than short term soil moisture field observations, or other fine scale soil attributes affecting transmission and disease such as pH and nitrogen content. This was successful in the Cairngorms, where adding area of cross-leaved heath, *Erica tetralix*, resulted in a very strong, positive, relationship with increasing area of symptoms (Δ DIC = 33), corroborating the response with increasing soil moisture as cross-leaved heath grows in constantly wet but not inundated soils (Hill et al., 2004). Managers of juniper populations in heathland habitats could use this result to prioritise detection surveys or identify unsuitable microsites for supplementary planting of juniper seedlings. Moreover, this finding suggests microsites most vulnerable to *P. austrocedri* infection in other habitats could be identified using indicator species with distinctive soil moisture preferences.

Uncoupling relationships between vegetative cover and soil moisture from other factors such as interspecific competition and land management practices proved more difficult for the remaining populations. The best Perthshire model was obtained by adding area of broad-buckler fern, *Dryopteris dilatata,* which increased with increasing area of symptoms (Δ DIC = 32, BCI did not bridge zero). This correlation is more likely to result from the fern preferentially colonising dead juniper following *P. austrocedri* induced mortality than suggest a higher percentage of symptoms occurred in the drier soil conditions favoured by the fern (Table 3) (Hill et al., 2004; Rünk et al., 2012). Adding area of brambles (*Rubus fruticosus* agg.) yielded the greatest improvement in Lake District model performance (Δ DIC = 56) and showed a strong (BCI 0.90 – 0.94), negative relationship with area of symptoms. While four other short-listed taxa for the Lake District also indicate lower soil moisture conditions (Hill et al., 2004), brambles are very palatable to both sheep and deer, indicating reduced herbivory where

present in quadrats (Harmer et al., 2010; Van Uytvanck and Hoffmann, 2009). Thus increasing symptoms in the absence of brambles might point to herbivore mediated dispersal of inoculum. A cost distance analysis comparing three cattle grazing scenarios (no grazing, roaming with intermittent barriers such as steep slopes and free roaming) found total area and dispersion of *P. austrocedri* was higher in Chilean cedar forests with unrestricted grazing (La Manna et al., 2013). Similarly, infection of Port-Orford cedar with *P. lateralis* increases along wildlife (including bear) trails that "fill-in" uninfected sites following disease establishment around creek edges (Jules et al., 2008). While our findings also implicate herbivores as potential vectors of inoculum between juniper stands, they clearly indicate that infection does not increase with direct herbivore damage, as this covariate was absent from both the Cairngorms and Lake District models and though present in Perthshire, symptoms decreased with increasing herbivory (BCI 0.90 – 0.94). However, overgrazing has long been implicated in the dramatic decline of UK juniper stands so a reduction in herbivore densities could not only improve the survival rates of existing populations and permit regeneration (Broome et al., 2017; Clifton et al., 1997; Thomas et al., 2007; Ward and Shellswell, 2017) but also reduce the risk of pathogen transmission.

Slope was present in all top models, explaining some of the residual variance with area of symptoms, even in the limited range occupied by the Cairngorms population (Table 2), but the weak evidence for these effects makes it difficult to interpret the precise nature of the relationship between slope and area of symptoms. We also detected weak relationships with area of berry-bearing juniper, evidenced by the presence of this covariate in all top models. However, again the direction of this effect was difficult to ascertain, with the exception of the Cairngorms population where there was weak support for a positive correlation (Table 7). The weak response could indicate female juniper without berries were missed by the survey. Similarly, juniper density was selected in all top models, and tended to show a weakly positive relationship with symptoms where evidence for the effect was stronger (Perthshire population, Table 5). Other studies of field scale infections, including that of Chilean cedar with

692 *P. austrocedri* and white oak (*Quercus alba*) with the similarly soil-borne *P. cinnamomi*, have
693 found symptom intensity to increase with increasing host density. The most likely explanations
694 for the absence of this relationship in our study are i) our characterisation of juniper density
695 as a binary measure of ± 20 % cover in 30 x 30 m was too simplistic, or ii) juniper density at
696 the 30 x 30 m scale was correlated with the area of juniper in 10 x 10 m, used to define the
697 number of trials in the models. We are currently exploring the role of host connectivity in
698 explaining site-level spread patterns over time, supported by empirical field studies of the
699 dispersal ability of the pathogen (Riddell et al., 2020) to better understand the mechanisms in
700 driving the spread of *P. austrocedri* at different spatial scales.
701
702 Models produced for Perthshire had the lowest accuracy (RMSE 42.59) despite containing the
703 largest number of covariates (11) meaning those included poorly account for the spatial
704 distribution of symptoms. The watercourses mapped for Perthshire include herringbone
705 drainage channels opened in 2011 (Taylor, H., 2019, pers. comm. 1 Nov) after juniper stands
706 started to decline in the late 1990's (Broome et al., 2008) but before isolation of *P. austrocedri*
707 in 2012 (Green et al., 2015). The drainage work may have inadvertently distributed the
708 pathogen across the site by disturbing watercourses and moving contaminated soil in tyre
709 treads. It is unclear if the very strong increase in area of symptoms with decreasing altitude
710 (BCI > 0.95) reflects the location where the pathogen was first introduced or the drainage
711 activity that was concentrated between 220 – 250 m of the 180 – 310 m altitudinal range (Fig.
712 3, Table 2) causing the pathogen to spread further and faster than dispersal through soil
713 moisture alone. This highlights the importance of capturing and integrating the spatial
714 arrangement and intensity of management actions into investigations of drivers of site level
715 variation in plant disease impacts (Fernández-habas et al., 2019).
716
717
718
719

5.0 Conclusion

Our study provides valuable insights about how conditions favouring newly invading plant diseases can be delineated by collecting and modelling spatially explicit data at field scale. Directly measuring covariates in the field in sites of different disease status, across key environmental gradients using a carefully designed sampling strategy, enabled us to explore a wide range of potential drivers, identify those with the most explanatory power and make comparisons between populations occupying different ranges along each gradient. Our findings can be used by practitioners to predict areas of increased and decreased infection risk and inform tangible local management inventions to prevent or reduce pathogen spread and aid the restoration or establishment of new juniper populations.

Interventions to manage juniper populations at local level such as drainage, grazing exclosures and seedling propagation require significant resources (Forestry Commission Scotland, 2006). The introduction of *P. austrocedri* to the UK risks this investment and the longevity of these actions if measures to prevent disease introduction and establishment are not undertaken. Our results suggest *P. austrocedri* is most likely to infect juniper where it occupies wet microsites - in the UK and across its global range. Therefore, surveys to detect *P. austrocedri* could initially target stands or populations occupying consistently wet microsites, identified with the aid of plant species indicators. Increased area of symptoms suggests inoculum is present in higher concentrations and that disturbance of soil and soil water in these microsites may pose a higher risk for pathogen translocation and spread. While improved biosecurity measures, such as cleaning all machinery, equipment and footwear before and after accessing juniper sites (irrespective of known disease status), will reduce the risk of pathogen introduction and spread (Department for Environment Food & Rural Affairs, 2014b), our findings further support recommendations published by the UK Department for Environment, Food and Rural Affairs in the Juniper Management Guidelines to divert footpaths away from waterlogged areas and only plant juniper in drier microsites, giving full

consideration to the vulnerability of existing populations, suspected disease status, soil type and the watercourse network (Department for Environment Food & Rural Affairs, 2017). Continued emphasis on improving the quality and extent of populations in drier soil conditions by regulating grazing levels, curtailing stand removal and creating spaces for natural regeneration (Broome et al., 2017; Wilkins and Duckworth, 2011) will help maximise resilience of native juniper populations to this new disease threat.

Acknowledgements

The authors wish to thank Rothiemurchus Estate, Dalemain Estate, Drummond Estate, the Steeles, and the Taylforths for permitting us to survey juniper populations they manage; Carolyn Riddell for assistance with qPCR analysis, as well as lesion sampling alongside April Armstrong and Ewan Purser; France Gerard and John Redhead for advice on aerial image classification methods; Hollie Cooper, Morag McCracken and Pete Scarlett for preparing and lending survey equipment; and finally to Fiona Cameron, Deborah Comyn-Platt, Etienne Duperron, Rory Hodd, Susan Medcalf, Denise Pallett, Mari Roberts and Rosamund Sparks for their excellent assistance collecting field data. F. Donald was funded by the Scottish Forestry Trust, Scottish Forestry, Forest Research, Scottish Natural Heritage and the Royal Botanic Garden Edinburgh. The manuscript was improved by two anonymous reviewers.

Appendix A. Mapping juniper study populations

Appendix B. Associate species target list

Appendix C. Distribution of *P. austrocedri* qPCR results

Appendix D. Additional information for model selection

771 **References**

772 Anderson, R.M., May, R.M., 1986. The invasion, persistence and spread of infectious
773 diseases within animal and plant communities. Philos. Trans. R. Soc. Lond. B. Biol. Sci.
774 314, 533–570. https://doi.org/10.1098/rstb.1986.0072
775 Baccalá, N.B., Rosso, P.H., Havrylenko, M., 1998. *Austrocedrus chilensis* mortality in the
776 Nahuel Huapi National Park (Argentina). For. Ecol. Manage. 109, 261–269.
777 https://doi.org/10.1016/S0378-1127(98)00250-3
778 Barwell, L.J, Perez-Sierra, A., Henricot, B., Harris, A., Burgess, T.I., Hardy, G., Scott, P.,
779 Williams, N., Cooke, D., Green, S., Chapman, D.S., Purse, B.V. (in review). Trait-based
780 approaches for predicting future global impacts of pathogens in the genus
781 *Phytophthora*.
782 Bjornstad, O.N., 2019. ncf: Spatial Covariance Functions. R package version 1.2-8.
783 https://CRAN.R-project.org/package=ncf
784 Botanical Society of Britain and Ireland, 2017. *Juniperus communis* records from live
785 database [WWW Document]. URL http://bsbi.org/maps?taxonid=2cd4p9h.8r1
786 (accessed 5.12.17).
787 Boyd, I.L., Freer-Smith, P.H., Gilligan, C.A., Godfray, H.C.J., 2013. The consequence of tree
788 pests and diseases for ecosystem services. Science 342, 823-833.
789 https://doi.org/10.1126/science.1235773
790 Broome, A., Holl, K., 2017. Can the site conditions required for successful natural
791 regeneration of juniper (*Juniperus communis* L.) be determined from a single species
792 survey? Plant Ecol. Divers. 00, 1–10. https://doi.org/10.1080/17550874.2017.1336186
793 Broome, A., Long, D., Ward, L.K., Park, K.J., 2017. Promoting natural regeneration for the
794 restoration of Juniperus communis: a synthesis of knowledge and evidence for
795 conservation practitioners. Appl. Veg. Sci. 1–13. https://doi.org/10.1111/avsc.12303
796 Broome, A, Hendry, S., Smith, M., Rayner, W., Nichol, B., Perks, M., Connolly, T., Tene, A.,
797 Bochereau, F., 2008. Investigation of the possible causes of dieback of Glenartney
798 Juniper Wood SAC Perthshire. Project No: 18895. Report commissioned by Scottish

799 Natural Heritage. Forest Research. Roslin.
800 Bunny, F.J.; Crombie, D.S.; Williams, M.R., 1995. Growth of lesions of *Phytophthora*
801 *cinnamomi* in stems and roots of jarrah (*Eucalyptus marginata*) in relation to rainfall and
802 stand density in mediterranean forest of Western Australia. Can. J. For. Res. 25, 961–
803 969.
804 Calı´, S.G., 1996. *Austrocedrus chilensis*: estudio de los anillos de crecimiento y su relacio´n
805 con la dina´mica del '"Mal del Ciprés"' en el P.N. Nahuel Huapi, Argentina. Universidad
806 Nacional del Comahue.
807 Chapman, D., Purse, B.V., Roy, H.E., 2017. Global trade networks determine the distribution
808 of invasive non-native species. Glob. Ecol. Biogeogr. 1–11. https://doi.org/10.1002/elan.
809 Chapman, D.S., Makra, L., Albertini, R., Bonini, M., Páldy, A., Rodinkova, V., Šikoparija, B.,
810 Weryszko-Chmielewska, E., Bullock, J.M., 2016. Modelling the introduction and spread
811 of non-native species: international trade and climate change drive ragweed invasion.
812 Glob. Chang. Biol. 22, 3067–3079. https://doi.org/10.1111/gcb.13220
813 Clifton, S.J., Ward, L.K., Ranner, D.S., 1997. The status of juniper - *Juniperus communis* L. -
814 in North-East England. Biol. Conserv. 79.
815 Cunniffe, N.J., Cobb, R.C., Meentemeyer, R.K., Rizzo, D.M., Gilligan, C.A., 2016. Modeling
816 when, where, and how to manage a forest epidemic, motivated by sudden oak death in
817 California. Proc. Natl. Acad. Sci. 113, 5640–5645.
818 https://doi.org/10.1073/pnas.1602153113
819 Department for Environment Food & Rural Affairs, 2017. Juniper management guidelines.
820 https://www.planthealthcentre.scot/sites/www.planthealthcentre.scot/files/inline-
821 files/JuniperManagementGuidelinesSeptember2017Published.pdf
822 Department for Environment Food & Rural Affairs, 2014a. Tree Health Management Plan.
823 https://assets.publishing.service.gov.uk/government/uploads/system/uploads/attachme
824 nt_data/file/307299/pb14167-tree-health-management-plan.pdf
825 Department for Environment Food & Rural Affairs, 2014b. Protecting Plant Health. A Plant
826 Biosecurity Strategy for Great Britain.

https://assets.publishing.service.gov.uk/government/uploads/system/uploads/attachment_data/file/307355/pb14168-plant-health-strategy.pdf

Dillon, W.W., Haas, S.E., Rizzo, D.M., Meentemeyer, R.K., 2014. Perspectives of spatial scale in a wildland forest epidemic. Eur. J. Plant Pathol. 138, 449–465. https://doi.org/10.1007/s10658-013-0376-3

El Mujtar, V.A., Perdomo, M.H., Gallo, L.A., Grau, O., 2012. Susceptibilidad diferencial al mal del ciprés entre sexos de *Austrocedrus chilensis* en la patagonia (Argentina). Bosque 33, 221–226. https://doi.org/10.4067/S0717-92002012000200012

[dataset] Farewell, T.S., Truckell, I.G., Keay, C.A., Hallett, S., 2011. Use and applications of the Soilscapes datasets. http://www.landis.org.uk/downloads/downloads/Soilscapes_Brochure.pdf

Fernández-Habas, J., Fernández-Rebollo, P., Rivas Casado, M., García Moreno, A.M., Abellanas, B., 2019. Spatio-temporal analysis of oak decline process in open woodlands: a case study in SW Spain. J. Environ. Manage. 248, 109308. https://doi.org/10.1016/j.jenvman.2019.109308

Forbes, A.R.D., 1984. Glen Artney Juniper Wood: An ecological study. Honours thesis (unpubl.). Stirling University, Stirling.

Forestry Commission Scotland, 2006. Support for juniper conservation under the Scottish Rural Development Programme (SRDP). https://scotland.forestry.gov.uk/images/corporate/pdf/junipersrdptechnicalnote.pdf

Gelman, A., Hill, J., 2006. Data analysis using regression and multilevel/hierarchical models. Cambridge University Press.

Gilligan, C.A., Van Den Bosch, F., 2008. Epidemiological models for invasion and persistence of pathogens. Annu. Rev. Phytopathol 46, 385–418. https://doi.org/10.1146/annurev.phyto.45.062806.094357

Grabs, T., Seibert, J., Bishop, K., Laudon, H., 2009. Modeling spatial patterns of saturated areas: a comparison of the topographic wetness index and a dynamic distributed model. J. Hydrol. 373, 15–23. https://doi.org/10.1016/j.jhydrol.2009.03.031

855 Green, S., Elliot, M., Armstrong, A., Hendry, S.J., 2015. *Phytophthora austrocedrae* emerges
856 as a serious threat to juniper (*Juniperus communis*) in Britain. Plant Pathol. 64, 456–
857 466. https://doi.org/10.1111/ppa.12253
858 Green, S., Hendry, S.J., Macaskill, G.A., Laue, B.E., Steele, H., 2012. Dieback and mortality
859 of *Juniperus communis* in Britain associated with *Phytophthora austrocedrae*. New
860 Disease Reports 26, 2. https://doi.org/10.5197/j.2044-0588.2012.026.002
861 Greslebin, A.G., Hansen, E.M., 2010. Pathogenicity of *Phytophthora austrocedrae* on
862 *Austrocedrus chilensis* and its relationship with mal del ciprés in Patagonia. Plant
863 Pathol. 59, 604–612. https://doi.org/10.1111/j.1365-3059.2010.02258.x
864 Greslebin, A.G., Hansen, E.M., Sutton, W., 2007. *Phytophthora austrocedrae* sp. nov., a
865 new species associated with *Austrocedrus chilensis* mortality in Patagonia (Argentina).
866 Mycol. Res. 111, 308–316. https://doi.org/10.1016/j.mycres.2007.01.008
867 Hansen, E.M., 2015. *Phytophthora* species emerging as pathogens of forest trees. Curr. For.
868 Reports 1, 16–24. https://doi.org/10.1007/s40725-015-0007-7
869 Hardham, A.R., 2005. *Phytophthora cinnamomi*. Mol. Plant Pathol. 6, 589–604.
870 https://doi.org/10.1111/j.1364-3703.2005.00308.x
871 Harmer, R., Kiewitt, A., Morgan, G., Gill, R., 2010. Does the development of bramble (*Rubus*
872 *fruticosus* L. agg.) facilitate the growth and establishment of tree seedlings in
873 woodlands by reducing deer browsing damage? Forestry 83, 93–102.
874 https://doi.org/10.1093/forestry/cpp032
875 Henricot, B., Pérez-Sierra, A., Armstrong, A.C., Sharp, P.M., Green, S., 2017. Morphological
876 and genetic analyses of the invasive forest pathogen *Phytophthora austrocedri* reveal
877 that two clonal lineages colonized Britain and Argentina from a common ancestral
878 population. Phytopathology 107, 1532–1540.
879 https://doi.org/10.1094/PHYTO-03-17-0126-R
880 Hijmans, R.J., 2016. raster: Geographic Data Analysis and Modeling. R package version
881 3.0-2. https://CRAN.R-project.org/package=raster
882 Hill, M.O., Preston, C.D., Roy, D.B., 2004. PLANTATT Attributes of British and Irish plants:

883 status, size, life history, geography and habitats. NERC Centre for Ecology and
884 Hydrology, Cambridge.
885 Hughes, G., Madden, L.V., 1993. Using the beta-binomial distribution to describe
886 aggregated patterns of disease incidence. Ecol. Epidemiol. 83, 759–763.
887 [dataset] James Hutton Institute, 2011. 1:250,000 Soil map (National soil map of Scotland).
888 https://www.hutton.ac.uk/learning/natural-resource-datasets/soilshutton/soils-maps-
889 scotland/download#soilmapdata
890 Jules, E.S., Kauffman, M.J., Ritts, W.D., Carroll, A.L., 2002. Spread of an invasive pathogen
891 over a variable landscape: a non-native root rot on Port Orford cedar. Ecol. Soc. of
892 America 83, 3167–3181.
893 https://doi.org/10.1890/00129658(2002)083[3167:SOAIPO]2.0.CO;2
894 Kopecký, M., Čížková, Š., 2010. Using topographic wetness index in vegetation ecology:
895 does the algorithm matter? Appl. Veg. Sci. 13, 450–459.
896 https://doi.org/10.1111/j.1654-109X.2010.01083.x
897 Kovacs, K., Václavík, T., Haight, R.G., Pang, A., Cunniffe, N.J., Gilligan, C.A., Meentemeyer,
898 R.K., 2011. Predicting the economic costs and property value losses attributed to
899 sudden oak death damage in California (2010-2020). J. Environ. Manage. 92, 1292–
900 1302. https://doi.org/10.1016/j.jenvman.2010.12.018
901 La Manna, L., Greslebin, A.G., Matteucci, S.D., 2013. Applying cost-distance analysis for
902 forest disease risk mapping: *Phytophthora austrocedrae* as an example. Eur. J. For.
903 Res. 132, 877–885. https://doi.org/10.1007/s10342-013-0720-3
904 La Manna, L., Matteucci, S.D., 2012. Spatial and temporal patterns at small scale in
905 *Austrocedrus chilensis* diseased forests and their effect on disease progression. Eur. J.
906 For. Res. 131, 1487–1499. https://doi.org/10.1007/s10342-012-0617-6
907 La Manna, L., Matteucci, S.D., Kitzberger, T., 2008. Abiotic factors related to the incidence
908 of the *Austrocedrus chilensis* disease syndrome at a landscape scale. For. Ecol.
909 Manage. 256, 1087–1095. https://doi.org/10.1016/j.foreco.2008.06.023
910 La Manna, L., Rajchenberg, M., 2004a. Soil properties and *Austrocedrus chilensis* forest

911 decline in Central Patagonia, Argentina. Plant Soil 263, 29–41.
912 https://doi.org/10.1023/B:PLSO.0000047723.86797.13
913 La Manna, L., Rajchenberg, M., 2004b. The decline of *Austrocedrus chilensis* forests in
914 Patagonia, Argentina: soil features as predisposing factors. For. Ecol. Manage. 190,
915 345–357. https://doi.org/10.1016/j.foreco.2003.10.025
916 Long, D., Williams, J., 2007. Juniper in the British uplands: the Plantlife juniper survey
917 results. Stirling.
918 Meentemeyer, R.K., Cunniffe, N.J., Cook, A.R., Filipe, J.A.N., Hunter, R.D., Rizzo, D.M.,
919 Gilligan, C.A., 2011. Epidemiological modeling of invasion in heterogeneous
920 landscapes: spread of sudden oak death in California (1990–2030). Ecosphere.
921 https://doi.org/10.1890/ES10-00192.1
922 Mills, P., Dehnen-Schmutz, K., Ilbery, B., Jeger, M., Jones, G., Little, R., MacLeod, A.,
923 Parker, S., Pautasso, M., Pietravalle, S., Maye, D., 2011. Integrating natural and social
924 science perspectives on plant disease risk, management and policy formulation. Philos.
925 Trans. R. Soc. B Biol. Sci. 366, 2035–2044. https://doi.org/10.1098/rstb.2010.0411
926 [dataset] Moore, R.V., Morris, D.G., Flavin, R.W., 2000. CEH digital river network of Great
927 Britain (1:50,000).
928 https://catalogue.ceh.ac.uk/documents/7d5e42b6-7729-46c8-99e9-f9e4efddde1d
929 Mulholland, V., Schlenzig, A., Macaskill, G.A., Green, S., 2013. Development of a
930 quantitative real-time PCR assay for the detection of *Phytophthora austrocedrae*, an
931 emerging pathogen in Britain. For. Pathol. 43, 513–517.
932 https://doi.org/10.1111/efp.12058
933 Nagle, A.M., Long, R.P., Madden, L. V., Bonello, P., 2010. Association of *Phytophthora*
934 *cinnamomi* with white oak decline in southern Ohio. Plant Dis. 94, 1026–1034.
935 https://doi.org/10.1094/PDIS-94-8-1026
936 O'Hanlon, R., Choiseul, J., Brennan, J.M., Grogan, H., 2018. Assessment of the eradication
937 measures applied to *Phytophthora ramorum* in Irish *Larix kaempferi* forests. For.
938 Pathol. 48, 2003–2010. https://doi.org/10.1111/efp.12389

939 Penczykowski, R.M., Parratt, S.R., Barrès, B., Sallinen, S.K., Laine, A.L., 2018. Manipulating
940 host resistance structure reveals impact of pathogen dispersal and environmental
941 heterogeneity on epidemics. Ecology 99, 2853–2863. https://doi.org/10.1002/ecy.2526
942 Peterson, E., Hansen, E., Kanaskie, A., 2014. Spatial relationship between *Phytophthora*
943 *ramorum* and roads or streams in Oregon tanoak forests. For. Ecol. Manage. 312, 216–
944 224. https://doi.org/10.1016/j.foreco.2013.10.002
945 Plantlife, 2015. The state of Scotland's juniper in 2015. Plantlife, Stirling.
946 Purse, B.V, Rogers, D.J., 2009. 16-Bluetongue virus and climate change. Bluetongue 343–
947 364. https://doi.org/10.1016/B978-0-12-369368-6.50020-4
948 R Core Team, 2018. R: A language and environment for statistical computing. R Foundation
949 for Statistical Computing. Vienna, Austria. URL https://www.R-project.org/.
950 R Core Team, 2017. R: A language and environment for statistical computing. R Foundation
951 for Statistical Computing. Vienna, Austria. URL https://www.R-project.org/.
952 Redondo, M.A., Boberg, J., Stenlid, J., Oliva, J., 2018. Contrasting distribution patterns
953 between aquatic and terrestrial *Phytophthora* species along a climatic gradient are
954 linked to functional traits. ISME J. 12, 2967–2980.
955 https://doi.org/10.1038/s41396-018-0229-3
956 Riddell, C.E., Dun, H.F., Elliot, M., Armstrong, A.C., Clark, M., Forster, J., Hedley, P.E.,
957 Green, S., 2020. Detection and spread of *Phytophthora austrocedri* within infected
958 *Juniperus communis* woodland and diversity of co-associated Phytophthoras as
959 revealed by metabarcoding . For. Pathol. e12602. https://doi.org/10.1111/efp.12602
960 Rodwell, J.S., 1991. British Plant Communities Volumes 1:5. Cambridge University Press,
961 Cambridge.
962 Rue, H., Martino, S., Chopin, N., 2009. Approximate Bayesian inference for latent Gaussian
963 models by using integrated nested Laplace approximations. J. R. Stat. Soc. Ser. B Stat.
964 Methodol. 71, 319–392. https://doi.org/10.1111/j.1467-9868.2008.00700.x
965 Rünk, K., Zobel, M., Zobel, K., 2012. Biological Flora of the British Isles:
966 *Dryopteris carthusiana*, *D. dilatata* and *D. expansa*. J. Ecol. 100, 1039–1063.

https://doi.org/10.1111/j.1365-2745.2012.01985.x

The Scottish Government, 2016. The Scottish plant health strategy 2016-2021. https://www.gov.scot/publications/scottish-plant-health-strategy/

[dataset] Scottish Natural Heritage, 2017. National Vegetation Classification. https://gateway.snh.gov.uk/natural-spaces/dataset.jsp?dsid=NVC

Sullivan, G., 2003. Extent and condition of juniper scrub in Scotland. Scottish Nat. Herit. Arch. Rep. No. 026, Inverness.

Tene, A., Broome, A., Connolly, T., 2007. Investigation of the possible causes of dieback of Glenartney Juniper Wood SAC Perthshire. Project No: 18895. Part 1: age structure analysis. Report commissioned by Scottish Natural Heritage. Forest Research, Roslin.

Thomas, P.A., El-Barghathi, M., Polwart, A., 2007. Biological Flora of the British Isles: *Juniperus communis* L. J. Ecol. 95, 1404–1440. https://doi.org/10.1111/j.1365-2745.2007.01308.x

Thompson, R.N., Gilligan, C.A., Cunniffe, N.J., 2018. Control fast or control smart: when should invading pathogens be controlled? PLoS Comput. Biol. 14, 1–21. https://doi.org/10.1371/journal.pcbi.1006014

Tippett, J.T., McGrath, J.F., Hill, T.C., 1989. Site and seasonal effects on susceptibility of *Eucalyptus marginata* to *Phytophthora cinnamomi*. Aust. J. Bot. 37, 481–490. https://doi.org/10.1071/BT9890481

Troy, A., Morgan Grove, J., O'Neil-Dunne, J., 2012. The relationship between tree canopy and crime rates across an urban–rural gradient in the greater Baltimore region. Landsc. Urban Plan. 106, 262–270. https://doi.org/10.1016/J.LANDURBPLAN.2012.03.010

Van der Wal, J., Falconi, L., Januchowski, S., Shoo, L., Storlie, C., 2014. SDMTools: Species Distribution Modelling tools: tools for processing data associated with species distribution modelling exercises. R package version 1.1-221.1. https://CRAN.R-project.org/package=SDMTools

Van Uytvanck, J., Hoffmann, M., 2009. Impact of grazing management with large herbivores on forest ground flora and bramble understorey. Acta Oecologica 35, 523–532.

https://doi.org/10.1016/j.actao.2009.04.001

Verheyen, K., Adriaenssens, S., Gruwez, R., Michalczyk, I.M., Ward, L.K., Rosseel, Y., Van den Broeck, A., García, D., 2009. *Juniperus communis*: victim of the combined action of climate warming and nitrogen deposition? Plant Biol. 11, 49–59. https://doi.org/10.1111/j.1438-8677.2009.00214.x

Walker, K.J., Stroh, P.A., Ellis, R.W., 2017. Threatened plants in Britain and Ireland. Botanical Society of Britain and Ireland, London.

Ward, L.K., Shellswell, C.H., 2017. Looking after juniper. Plantlife, Salisbury.

Werres, S., Elliot, M., Greslebin, A.G., 2014. Plant diseases and diagnosis JKI Data Sheets 1–13. https://doi.org/10.5073/jkidspdd.2014.001

Whittome, T., 2010. Report No CASL-0909-129-1a Glenartney Juniper Wood Aerial Photography 2010. Report commissioned by Scottish Natural Heritage, Inverness.

Wilkins, T.C., Duckworth, J.C., 2011. Breaking new ground for juniper - a management handbook for lowland England. Plantlife, Salisbury.

Zeileis, A., Grothendieck, G., 2005. zoo: S3 infrastructure for regular and irregular time series. J. Stat. Softw. 14, 1–27. https://doi.org/10.18637/jss.v014.i06

Mapping juniper study populations

To identify sampling locations along a gradient of juniper density, juniper distribution maps were first required for each population.

A.1.1 Distribution mapping of the Perthshire juniper population

A map of the Perthshire population was created from a classification of imagery collected and processed by Caledonian Air Surveys Ltd (Whittome, 2010) under contract to Scottish Natural Heritage (SNH). Full colour (RGB) and false colour infrared (CIR) imagery was collected in August 2010 at 15 cm resolution from a light aircraft using a 50-megapixel Hasselblad H4D-50 digital camera (Whittome, 2010). Maximum likelihood (ML) classification of the resulting imagery was implemented in the Focus program included in Geomatica version 9.1.7-R5 (PCI Geomatics, 2010). The classification used five object classes: asymptomatic juniper, dead juniper, trees, bracken and other. The spectral signature space occupied by each object class is assigned a multivariate Gaussian distribution, with a mean and covariance matrix fit for each class from sets of training pixels (Richards, 1999). Each pixel in the image is then assigned by the ML classifier to the object class with the highest likelihood (Environmental Systems Research Institute, 2016). No information about the number of training pixels used for classification or the resulting classification accuracy was supplied (Whittome, 2010). Two shapefiles of juniper, classified as asymptomatic or dead, were produced and made available to the authors by SNH. We joined the shapefiles in R version 3.4.0 (R Core Team, 2017) and converted it to a raster, resampled to 1 m resolution (i.e. the minimum unit of juniper increased from 0.15 m^2 to 1 m^2) using the *rasterize* function in the raster package (Hijmans, 2016) implemented with a mean function. The raster was then overlain with a 10 x 10 m grid created from 5 m digital elevation models (DEM) supplied by NeXTPerspectives™ (updated February 2014), averaged to 10 m using the *aggregate* function in the raster package (Hijmans, 2016).

A.1.2 Distribution mapping of the Lake District and Cairngorms juniper populations

No pre-existing spatial information was available for the Lake District or Cairngorms juniper populations, so we used ARC GIS v. 10.5 (Environmental Systems Research Institute, 2017) to carry out a supervised ML classification of full colour (RGB), 25 cm imagery collected in 2010 and supplied by NeXTPerspectives™. One image was provided for each location, which was aligned and clipped to the boundary of the corresponding juniper population then classified using the ML method described above. A dataset of pixels representing different observable object classes was created for each image and partitioned into a training set and a test set at a ratio of 80:20 pixels (Table A.1). As few *P. austrocedri* symptoms were visible across either population in 2010, separation of asymptomatic and symptomatic juniper object classes was not required for classification.

Table A.1. List of object classes, number of training and test pixels used to classify 25 cm RGB images of the Lake District and Cairngorms juniper populations.

Population	Object classes	Training	Test
Lake District	Juniper	54000	10800
	Trees	47271	9454
	Tree shadow	496	99
	Rock	1514	303
	Other	156124	31225
Cairngorms	Juniper	35057	7011
	Trees	121016	24203
	Tree shadow	6643	1329
	Rock	6060	1212
	Bracken	5881	1176
	Grass	56072	11214
	Heath	62335	12467

Classification was performed using the *create signatures* and *maximum likelihood classification* tools in the spatial analyst toolbox. The value of each pixel in the test dataset was extracted from the classified image using *extract* in the raster package (Hijmans, 2016) implemented in R. version 3.4.0 (R Core Team, 2017). Confusion matrices were used to summarise the probability of correctly assigning test pixels to object classes (Table A.2). Commission is the number of pixels incorrectly included in an object class whereas omission

is the number of pixels incorrectly missed out; user's accuracy is 1 - commission error and producer's accuracy is 1 - omission error. Cohen's kappa statistic was calculated using the *accuracy* function in the rfUtilities package (Evans et al., 2011) as a commonly used metric to interpret test pixel classification accuracy, accounting for both commission and omission errors and correcting overall prediction accuracy by the accuracy expected to occur by chance (Allouche et al., 2006). The following indicative kappa thresholds were suggested by Landis and Koch (1977): 0.41 – 0.6 moderate, 0.61 – 0.8 substantial and > 0.81 almost perfect.

As the kappa statistics for juniper classification met the threshold for "moderate" and "substantial" classification accuracy in the Cairngorms and Lake District populations respectively, the analysis was considered sufficiently accurate at the time to identify potential sampling locations described in the quadrat stratification section in the methods.

The resulting rasters of juniper distribution were then resampled to 1 m resolution and overlain with a 10 x 10 m grid using the same methods described for the Perthshire population.

Table A.2. Confusion matrix presenting rates of omission and commission, user's and producer's accuracies per object class obtained from the ML classification of the 25 cm RGB imagery supplied by Next Perspectives™ of a) the Lake District b) the Cairngorms juniper study populations.

a)

		Reference					Total	User's	Commission	Kappa
		Juniper	Trees	Tree shadow	Rock	Other				
Predicted	Juniper	7655	441	35	70	2969	11170	0.69	0.31	0.62
	Trees	758	8388	14	0	847	10007	0.84	0.16	0.83
	Tree shadow	260	219	49	3	244	775	0.06	0.94	0.11
	Rock	543	1	1	190	6198	6933	0.03	0.97	0.04
	Other	1584	405	0	40	20967	22996	0.91	0.09	0.54
	Total	10800	9454	99	303	31225				
	Producer's	0.71	0.89	0.49	0.63	0.67				
	Omission	0.29	0.11	0.51	0.37	0.33				

b)

		Reference							Total	User's	Commission	Kappa
		Juniper	Trees	Tree shadow	Rock	Bracken	Grass	Heath				
Predicted	Juniper	4483	2489	0	2	0	469	2712	10155	0.44	0.56	0.44
	Trees	2210	20981	11	0	0	785	0	23987	0.87	0.13	0.80
	Tree shadow	0	604	1311	0	0	0	0	1915	0.68	0.32	0.99
	Rock	0	0	0	1197	7	0	10	1214	0.99	0.01	0.81
	Bracken	0	0	0	1	1149	0	0	1150	1.00	0.00	0.99
	Grass	17	120	0	3	11	9601	1	9753	0.98	0.02	0.90
	Heath	301	9	7	9	9	359	9744	10438	0.93	0.07	0.44
	Total	7011	24203	1329	1212	1176	11214	12467				
	Producer's	0.64	0.87	0.99	0.99	0.98	0.86	0.78				
	Omission	0.36	0.13	0.01	0.01	0.02	0.14	0.22				

A.1.3 Revised distribution mapping of the Lake District juniper population

Concerned that inaccuracy in the image classification may lead to errors in proportional sampling of the eight juniper density categories, we wanted to compare the density distribution of sampled quadrats to those derived from the original, and an improved, image classification. The quality of the Cairngorms image was insufficient to make re-analysis practicable but the opportunity arose to re-classify the Lake District image using ARC GIS v.10.5 after fieldwork was completed. We addressed the uneven illumination by separating the image, by eye, into five different sections with different depths of shadow and developing sets of 70 training to 30 test pixels unique to each section (Table A.3). Multiple studies have shown maximum likelihood classification of land cover is outperformed by using the random forest (RF) algorithm (Attarchi and Gloaguen, 2014; Khatami et al., 2016; Waske and Braun, 2009). We implemented the algorithm using the *random trees* tool in the spatial analyst toolbox. Maximum number of trees was set to 200, maximum tree depth to 50 and maximum number of samples per class to 1000. The resulting ESRI classification definition file was then loaded in the *classify raster* tool in the spatial analyst toolbox to produce classified rasters of each image section, assessed using confusion matrices and kappa as outlined in S.1.2. Once the best classification of juniper according to the accuracy statistics (minimum kappa of 0.7) was obtained for each section, the classified image sections were mosaiced back together for the remaining processing.

Predicted juniper pixels isolated from any other juniper pixels in eight neighbouring directions were identified and deleted using the *freq* function in the raster package (Hijmans, 2019) implemented in R v. 3.5.2 (R Core Team, 2018). Juniper pixels visible in the centre of deciduous tree crowns were then manually deleted. These operations deleted 0.05 % juniper pixels identified by the classifier.

Table A.3. List of object classes and total number of pixels used to train the RF algorithm and test the result of the classification of 25 cm RGB image of the Lake District juniper population.

Class	Training	Test
Juniper	17747	7606
Trees	36782	15764
Tree shadow	9369	4041
Rock	15231	6528
Bracken	49218	21092
Grass	9541	4158
Heath	1828	784

Compared to the original Lake District image analysis, the revised classification of juniper improved by 0.13 kappa units keeping it within the range for substantial classification accuracy (Table A.4). Where the original classification predicted 29 % more juniper pixels than the number observed, the revised classification predicted 15 % fewer juniper pixels (Table A.2a, Table A.4). User's accuracy improved to 82 % reducing the number of pixels incorrectly classified as juniper by 13 % and producer's accuracy improved to 74 % increasing the number of pixels correctly classified as juniper by 3 % (Table A.2a, Table A.4). The largest proportion of pixels mistakenly identified as juniper were donated from the "tree shadow" category (10 %) and the greatest percentage of misidentified juniper pixels were predicted to be grass (9 %).

Table A.4. Confusion matrix presenting rates of omission and commission, user's and producer's accuracies per object class obtained from the RF revised classification of the 25 cm RGB image supplied by Next Perspectives™ of the Lake District juniper population.

		Reference							Total	User's	Commission	Kappa
		Juniper	Trees	Tree shadow	Rock	Bracken	Grass	Heath				
Predicted	Juniper	5626	396	668	80	61	42	17	6890	0.82	0.18	0.75
	Trees	503	13474	100	4	987	344	0	15412	0.87	0.13	0.82
	Tree shadow	275	116	3187	12	12	0	14	3616	0.88	0.12	0.82
	Rock	57	43	50	5641	1183	34	6	7014	0.8	0.2	0.82
	Bracken	303	52	5	605	17537	478	5	18985	0.92	0.08	0.81
	Grass	667	1660	19	34	1305	3251	0	6936	0.47	0.53	0.55
	Heath	175	23	17	12	8	0	742	977	0.76	0.24	0.84
	Total	7606	15764	4046	6388	21093	4149	784				
	Producer's	0.74	0.85	0.79	0.88	0.83	0.78	0.95				
	Omission	0.26	0.15	0.21	0.12	0.17	0.22	0.05				

Pixels classified as juniper in the revised image were subset to a new raster, then resampled to 1 m using *rasterize* in the raster package (Hijmans, 2016) implemented with a mean function. The same method outlined in the quadrat stratification section was used to calculate the area of juniper at 10 x 10 and 30 x 30 m scales for each cell and then assign it to one of the eight juniper density categories (Table A.5). The ML analysis identified 10795 10 x 10 m cells containing juniper, compared to 8399 in RF classification. The proportion of cells distributed across density categories were comparable between the original and revised classifications (Figure A.1, Table A.5). Few cells were found in categories with dense 10 x 10 m but sparse 30 x 30 m cover (categories 3-4), or sparse 10 x 10 m and dense 30 x 30 m cover (category 5). The greatest proportion of cells were allocated to categories 7-8 with high % cover at both scales but the category with the highest proportion of cells differed by method. The sum of the area of juniper calculated at 10 x 10 m and 30 x 30 m for each juniper cell is highly correlated (Pearson $r^2 = 0.69$) between the two classifications. Comparing the sample distribution to that of the revised image classification suggests too many quadrats were sampled at high juniper density (category 8) but this may arise from the slight under-prediction of juniper occurrence in the revised image classification (Table A.4). The sample distribution does match the revised classification well in the lower density categories (Figure A.1), so we are satisfied that juniper sampling based on the original image classification was roughly proportional to the juniper density actually present across the site.

Table A.5. Description of the eight juniper density categories based on % juniper cover in 10 x 10 m quadrats and the 30 x 30 m including each quadrat, the percentage of cells allocated to each category following classification of 1 m resolution RGB imagery supplied by Next Perspectives™ using ML (original) and RF (revised) algorithms and the percentage of cells sampled by the field survey in each category.

Density category	% juniper cover		% 10 x 10 m cells per category		
	30 x 30 m	10 x 10 m	Original	Revised	Sample
1	0 - 20	1 – 10	9	14	11
2		11 – 25	5	13	11
3		26 – 50	1	2	0
4		50 - 100	0	0	0
5	21 - 100	1 – 10	3	4	0
6		11 – 25	12	15	13
7		26 – 50	28	29	26
8		50 - 100	42	23	39

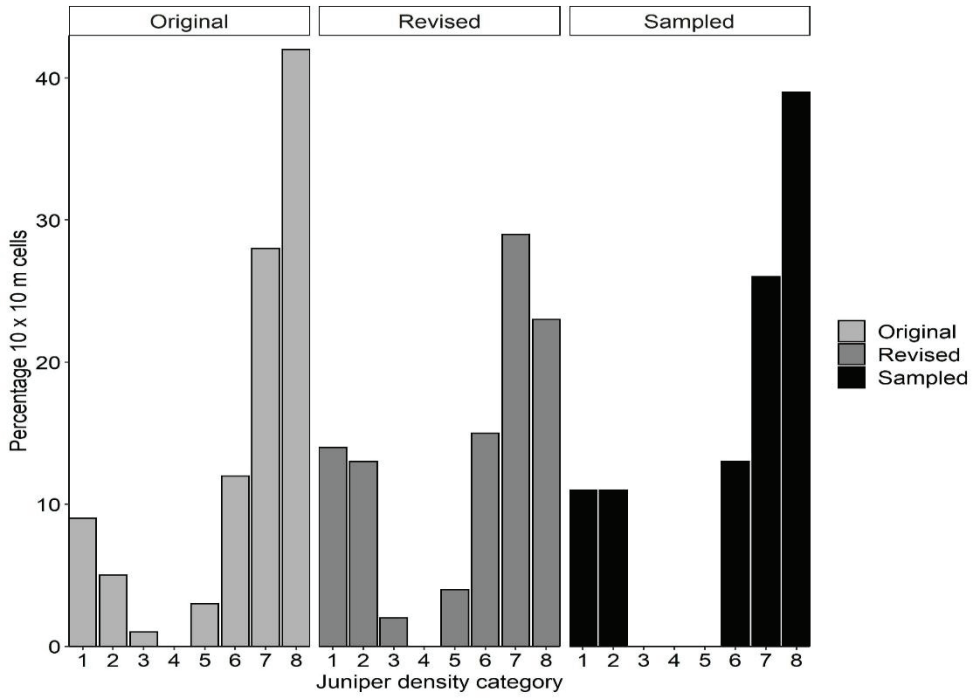

Figure A.1. Distribution of 10 x 10 m cells in the Lake District study area across eight juniper density categories (Table A.5) comparing the classification of 1 m resolution RGB imagery supplied by Next Perspectives™ using the original (ML) and revised (RF) methods and the percentage of cells sampled by the field survey. The number of 10 x 10 m cells containing juniper compared is 10795 (original), 8399 (revised), 46 (sampled).

References

Allouche, O., Tsoar, A., Kadmon, R., 2006. Assessing the accuracy of species distribution models: prevalence, kappa and the true skill statistic (TSS). J. Appl. Ecol. 43, 1223–1232. https://doi.org/10.1111/j.1365-2664.2006.01214.x

Attarchi, S., Gloaguen, R., 2014. Classifying complex mountainous forests with L-Band SAR and landsat data integration: a comparison among different machine learning methods in the Hyrcanian forest. Remote Sens. 6, 3624–3647. https://doi.org/10.3390/rs6053624

Environmental Systems Research Institute, 2017. ArcGIS Desktop, version 10.5. Redlands, CA.

Environmental Systems Research Institute, 2016. How maximum likelihood classification works [WWW Document]. URL http://desktop.arcgis.com/en/arcmap/10.3/tools/spatial-analyst-toolbox/how-maximum-likelihood-classification-works.htm

Evans, J.S., Murphy, M.A., Holden, Z.A., Cushman, S.A., 2011. Modeling species distribution and change using Random Forests, in: Drew, C.A., Wiersma, Y.F., Huettmann, F. (Ed.), Predictive Species and Habitat Modeling in Landscape Ecology: Concepts and Applications. New York, pp. 139–159.

Hijmans, R.J., 2016. raster: geographic data analysis and modeling. R package version 3.0-2. https://CRAN.R-project.org/package=raster

Khatami, R., Mountrakis, G., Stehman, S.V., 2016. A meta-analysis of remote sensing research on supervised pixel-based land-cover image classification processes: general guidelines for practitioners and future research. Remote Sens. Environ. 177, 89–100. https://doi.org/10.1016/j.rse.2016.02.028

Landis, J.R., Koch, G.G., 1977. The measurement of observer agreement for categorical data. Biometrics 33, 159–174. https://doi.org/10.2307/2529310

PCI Geomatics, 2010. Geomatica version 9.1.7-R5. Markham, Canada.

R Core Team, 2018. R: A language and environment for statistical computing. R Foundation for Statistical Computing. Vienna, Austria. URL https://www.R-project.org/.

R Core Team, 2017. R: A language and environment for statistical computing. R Foundation for Statistical Computing. Vienna, Austria. URL https://www.R-project.org/.

Richards, J.A., 1999. Remote sensing and digital image analysis: an introduction, 2nd ed. Springer Berlin, Heidelberg.

Waske, B., Braun, M., 2009. Classifier ensembles for land cover mapping using multitemporal SAR imagery. ISPRS J. Photogramm. Remote Sens. 64, 450–457. https://doi.org/10.1016/j.isprsjprs.2009.01.003

Whittome, T., 2010. Report No CASL-0909-129-1a Glenartney juniper wood aerial photography 2010. Report commissioned by Scottish Natural Heritage, Inverness.

Associate species target list

Table B.1. List of 42 target vascular plant species to record in 10 x 10 m quadrats categorised using Ellenberg moisture (F), reaction (R) and nitrogen (N) values given in Hill, Preston, & Roy (2004).

Vascular plant taxon	Soil pH & fertility			Soil moisture		
	Highly acidic (R = 2), nutrient poor (N = 1-2)	Slightly acidic (R = 3-5), moderately fertile (N = 3-5)	Neutral (R = 6-7), fertile (N = 6)	High moisture (F = 8-9)	Moderate moisture (F = 6-7)	Lower moisture (F = 5)
Erica tetralix	x			x		
Calluna vulgaris	x				x	
Empetrum nigrum	x				x	
Pinus sylvestris	x				x	
Vaccinium myrtillus	x				x	
Arctostaphylos uva-ursi	x					x
Erica cinerea	x					x
Vaccinium vitis-idaea	x					x
Betula pendula		x				x
Fagus sylvatica		x				x
Ilex aquifolium		x				x
Luzula sylvatica		x				x
Pteridium aquilinum		x				x
Quercus robur		x				x
Rubus fruticosus agg.		x				x
Taxus baccata		x				x
Ulex europaeus		x				x
Alnus glutinosa			x	x		
Iris pseudacorus			x	x		
Fraxinus excelsior			x		x	
Acer pseudoplatanus			x			x
Coryllus avellana			x			x
Crataegus monogyna			x			x
Hedera helix			x			x
Ulmus glabra			x			x
Molinia caerulea				x		
Myrica gale				x		
Salix cinerea				x		
Athyrium filix-femina					x	
Betula pubescens					x	
Deschampsia cespitosa					x	
Dryopteris affinis					x	
Dryopteris dilitata					x	
Dryopteris filix-mas					x	
Juncus conglomeratus					x	
Juncus effusus					x	
Lonicera periclymenum					x	
Oreopteris limbosperma					x	
Quercus petraea					x	
Sorbus aucuparia					x	

Distribution of *P. austrocedri* qPCR results

Tissue from lesions symptomatic for *P. austrocedri* was collected from juniper with foliage symtpoms within field quadrats and tested for *P. austrocedri* DNA using qPCR. Positive results were obtained for 49 % of quadrats in Perthshire, 58 % in the Lake District and 60 % in the Cairngorms (Table C.1), distributed across the full extent of each juniper population (Figure C.1). Symptomatic lesions were not found in the remaining quadrats, with the exception of three quadrats (5 %) in Perthshire and three (6 %) in the Lake District, where the presence of DNA was not positively confirmed by qPCR (Table C.1, Figure C.1). Inability to detect lesions on dead trees explains the inverse relationship between the percentage of quadrats with positive qPCR results and the area of symptoms detected across each study population (Figure 3, Table 2).

Table C.1**.** Comparison of the numbers of quadrats, lesion samples, positive and “not detected” qPCR results for *P. austrocedri* DNA for each study population. No detection of *P. austrocedri* occurs where symptomatic lesions could not be found within quadrats or where qPCR did not confirm DNA presence.

Measurement	Perthshire	Lake District	Cairngorms
Number of 10 x 10 m quadrats surveyed	51	48	50
Number of lesion samples collected	28	31	30
Number of quadrats where *P. austrocedri* present	25	28	30
Number of quadrats where *P. austrocedri* not detected	26 (3)	20 (3)	20 (0)

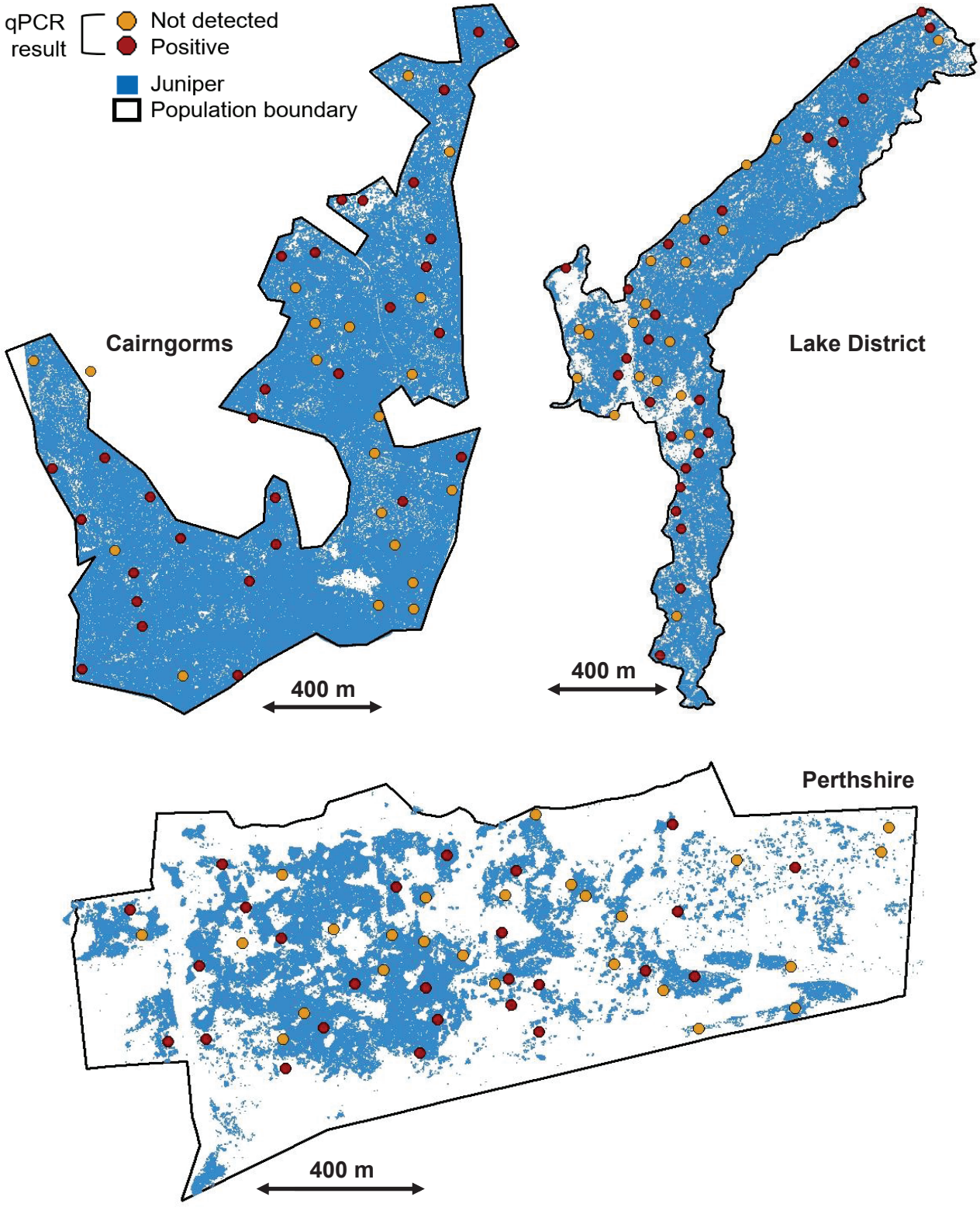

Figure C.1: Spatial distribution of qPCR results obtained from lesions symptomatic for *P. austrocedri* collected from 10 x 10 m quadrats at each study population.

Additional information for model selection

D.1 Correlations between environmental covariates

Correlations between all covariates investigated in the Perthshire, Lake District and Cairngorms juniper populations were investigated (Figure D.1). The dependent variable “Symptoms” (area of symptomatic juniper in 10 x 10 m) and the independent variable “Area” (area of juniper in 10 x 10 m) were included in the analysis but collinearity was only examined between the covariates (Figure D.1). No covariates were correlated with a Pearson r^2 value ≥ 0.6.

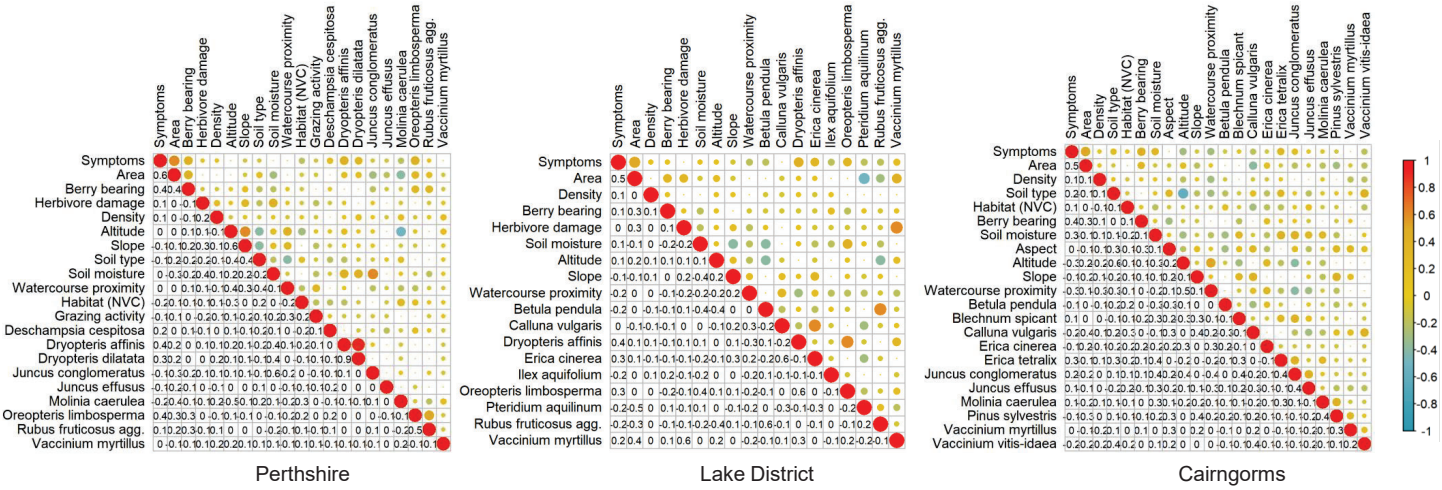

Figure D.1: Correlation plot between all investigated metrics for the Perthshire, Lake District and Cairngorms juniper populations. Pearson r^2 values are shown using colour scale and text to 1 decimal place. Covariate descriptions and units of measurement are given on Table 1.

D.2. Accounting for spatial autocorrelation in model residuals

Correlations in the residuals generated from beta-binomial GLMMs were calculated using Moran's I statistic. Positive spatial autocorrelation of the residuals was rarely significant in any of the top models for any of the populations up to the first 1000 m of inter-quadrat distance (Figure D.2).

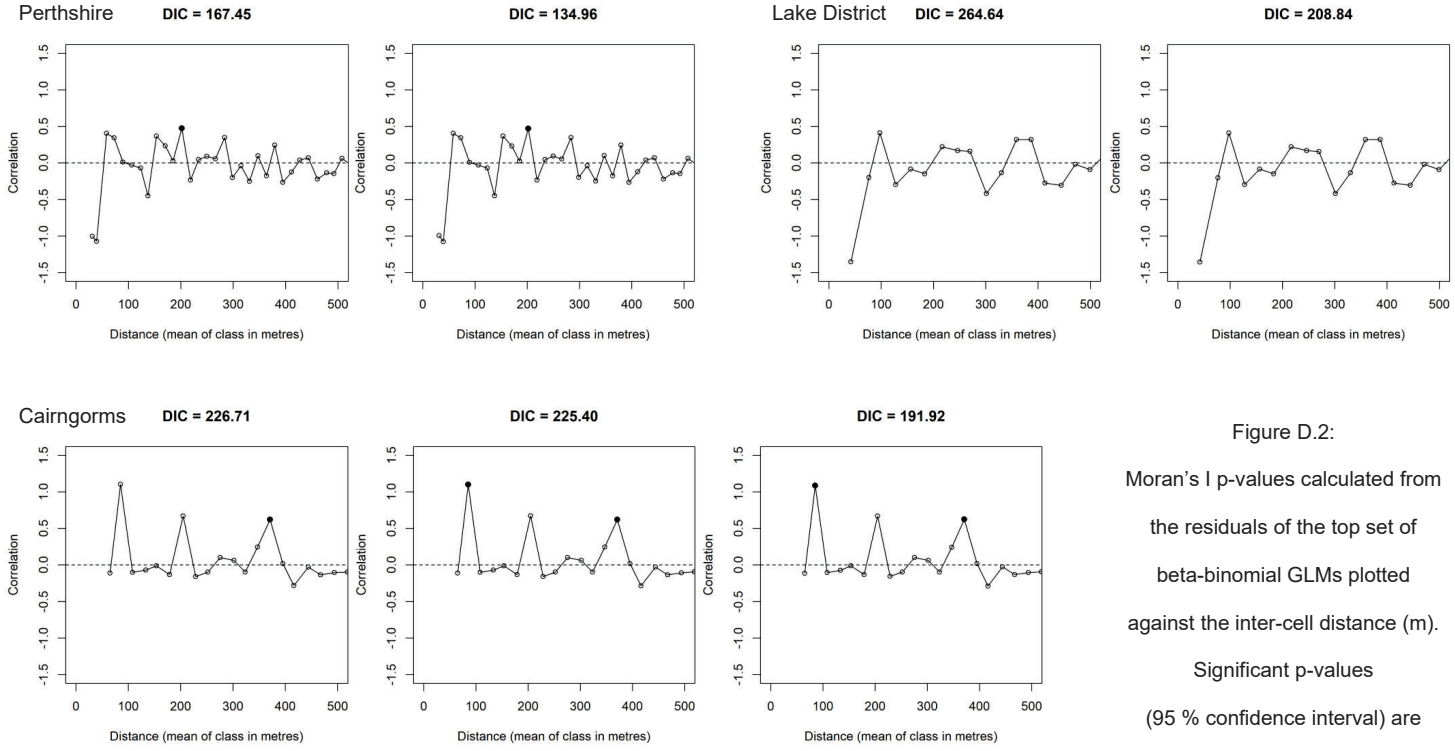

Figure D.2: Moran's I p-values calculated from the residuals of the top set of beta-binomial GLMs plotted against the inter-cell distance (m). Significant p-values (95 % confidence interval) are shown in black.